The Rhizobial effector NopT targets Nod factor receptors to regulate symbiosis in *Lotus japonicus*

Hanbin Bao[1], Yanan Wang[1], Haoxing Li[1], Qiang Wang[1], Yutao Lei[1], Ying Ye[1], Syed F. Wadood[2], Hui Zhu[1], Christian Staehelin[2], Gary Stacey[3], Shutong Xu[1], Yangrong Cao[1*]

[1] National Key Lab of Agricultural Microbiology, Hubei Hongshan Laboratory, Huazhong Agricultural University, Wuhan, Hubei, 430070, China

[2] State Key Laboratory of Biocontrol and Guangdong Key Laboratory of Plant Resources, School of Life Sciences, Sun Yat-sen University, East Campus, 510006 Guangzhou, China

[3] Divisions of Plant Science and Technology and Biochemistry, Christopher S. Bond Life Sciences Center, University of Missouri, Columbia, MO 65211, USA

* Corresponding author: Yangrong Cao, email: yrcao@mail.hzau.edu.cn

Short title: NopT associates with NFR1 and NFR5 to regulate symbiosis

Keywords: Legume–rhizobial symbiosis; rhizobial effector; Nod Factor Receptors; NopT.

One-sentence summary: The rhizobial effector NopT forms a mutual interaction with plant's two Nod factor receptors, NFR1 and NFR5, to precisely regulate rhizobial symbiosis in *Lout japonicus*

Abstract

It is well-studied that type-III effectors are essential required by gram-negative pathogens to directly target different cellular pathways from hosts, thus enhancing bacterial infection. However, in the unique context of legume-rhizobium symbiosis, the role of rhizobial effectors in regulating plant symbiotic pathways remains a subject of hypothesized understanding. Here, we show that NopT, a YopT-type cysteine protease from *Sinorhizobium fredii* NGR234 that could directly target symbiotic signaling pathway by associating with two plants' Nod factor receptors (NFR1 and NFR5). NopT inhibits cell death triggered by co-overexpression of NFR1/NFR5 in *Nicotiana benthamiana*. NopT interacts with both NFR1 and NFR5. NopT proteolytically cleaves NFR5 in both *in vitro* and *in vivo* assays, but is later inactivated *via* phosphorylation by NFR1. NopT plays an essential role in mediating rhizobial infection in *L. japonicus*. The truncated NopT, lacking 50 N–terminal amino acids post-autocleavage, retains the ability to cleave NFR5 but no longer interacts with NFR1. Intriguingly, certain *Sinorhizobium* species exclusivley harbor this truncated NopT in their genomes. These findings unveil an intricate regulatory interplay between rhizobia and legumes, wherein rhizobial NopT actively cleaves NFR5, and this cleavage process is subsequently suppressed following NopT phosphorylation by NFR1. This discovery presents a compelling narrative of a nuanced regulatory interplay between rhizobia and legumes, highlighting rhizobial effector as a direct mediator targeting symbiotic pathway from plants.

Introduction

The legume–rhizobial symbiosis stands as one of the most crucial and intricate mutualistic interactions in nature. Its significance extends beyond the supply of the substantial amount of ammonium provided by rhizobia, influencing plant growth and ecosystem sustainability, to serving as a pivotal model for investigating plant–microbe interactions (Yang et al., 2022). The orchestration of this symbiosis involves the perception of small molecules,

such as nod factors (NFs) and surface polysaccharides (Madsen et al., 2003; Kawaharada et al., 2015), along with the secretion of proteins, inlcuding the type three secretion system (T3SS) effectors, to regulate legume–rhizobial symbiosis (Sugawara et al., 2018; Zhang et al., 2021).

A receptor heterocomplex, consisting of two Lysin–motif receptor kinases (LYKs), plays a central role in recognizing various polysaccharide molecules. In nonlegumes like Arabidopsis, AtLYK5 and AtCERK1 (Chitin elicitor receptor kinase) are required for perception of chitin, triggering plant immunity to combat fungal pathogens (Cao et al., 2014). Conversely, in legumes, structurally similar receptors like *L. japonicus* NF receptor1 (LjNFR1) and LjNFR5 are vital for recognizing rhizobial lipo–chitooligosaccharide NF, initiating symbiotic signaling transduction (Broghammer et al., 2012; Bozsoki et al., 2017). The intricate regulation of NFRs is highlighted by the instances of hypersensitive cell death induced by their simultaneous overexpression in *Nicotiana benthamiana* leaves (Madsen et al., 2011) and defense–like responses in *Medicago truncatula* nodules upon overexpression of MtNFP (Nod factor perception, the ortholog of NFR5) (Moling et al., 2014), perhaps reflecting potential conservation of the plant LYK receptors in interactions with both pathogens and symbionts. Therefore, the protein abundance of NFRs must be tightly controlled to avoid this resistance response, allowing rhizobial infection to proceed, emphasizing the need for tight control to enable rhizobial infection.

T3SS effectors play a critical role in suppressing pattern–triggered immunity (PTI) during pathogen infections in plants (Jones and Dangl, 2006; Schubert et al., 2020). To avoid diseases, specific resistance (R) genes are employed to recognize successful avirulence (Avr) effectors which enable pathogens overcome PTI, known as effector-triggered immunity (ETI), a much stronger immnune

response combined with programmed cell death (Jones and Dangl, 2006). However, in contrast to the well-studied fucntion of Avr effectors from phytopathogenic bacteria in mitigating immunity by different mechanisms, how these effectors from symbiotic bacteria might contribute to mutualistic interaction is largely unknown.

Some effectors, such as YopT-type cysteine protease family, including *Pseudomonas* AvrPphB, *Yersinia* YopT, and *Rhizobial* NopT, are well conserved across different bacteria. AvrPphB from *Pseudomonas syringae* can directly proteolytically cleaves Arabidopsis receptor-like cytoplasmic kinase (RLCK) family proteins including PBS1, PBS1-like proteins, and BIK1, to suppress PTI (Zhang et al., 2010). While, the cleavage of PBS1 serves as a "decoy" in activating RPS5 (RESISTANCE TO PSEUDOMONAS SYRINGAE5)–mediated ETI (Shao et al., 2003b). *Yersinia* YopT directly cleaves Rho family leading to their inactivation to disrupt actin cytoskeleton of host cells (Shao et al., 2003b; Shao et al., 2003a). While, in *rhizobium* species, NopT have a dual function in regulating symbiosis. The exogenous expression of NopT from *Sinorhizobium fredii* NGR234 in *S. fredii* USDA257 almost blocks nodulation in soybean Nanfeng 15 but not other soybean cultivars (Khan et al., 2022), implying that NopT might act as an Avr effector. However, NopT positively regulates nodule formation in the interaction betwen *S. fredii* HH103 and soybean Suinong 14 (Li et al., 2023). NopT from *Bradyrhizobium* sp. ORS3257 promotes rhizobial infection in nodules of *Aeschynomene indica* (Teulet et al., 2019). Despite this, little is understood about how NopT precisely modulates rhizobial infection and the variations among NopTs from different rhizobia strains.

The challenge in studying rhizobial effectors lies in the availability of suitable assays by which to characterize their phenotypes. In this study, we capitalized on the observation that

ectopic expression of NFR1 and NFR5 in *N. benthamiana* leaves induces programed cell death (Madsen et al., 2011), a response that might be modulated by rhizobial effectors. Among the 15 known T3SS effector proteins encoded within the *S. fredii* NGR234 genome, only NopT, a homolog of the pathogenic effectors, YopT and AvrPphB (Shao et al., 2002; Dai et al., 2008), could specifically suppress this cell death response. This suggests that NopT might be an effector associated with NFRs. Our findings demonstrate that NopT interacts with both NFR1 and NFR5 at the plasma membrane, and cleaves NFR5 proteolytically at the juxtamembrane position to suppresses NF–mediated physiological responses. Perhaps as a means to regulate NopT activity, NFR1 phosphorylates intact NopT, inactivating its protease activity. However, the autocleaved NopT retains the ability to cleave NFR5 but loses its association with NFR1. Intriguingly, some *Sinorhizobium* species possess only the truncated versions of NopT (relative to NGR234 NopT) that might evade suppression by NFR1. This study enveils a distinct and mutual regulatory model, in which the rhizobial effector NopT directly targets NFR5 to suppress symbiotic signaling, and NFR1-mediated phosphorylation acts as a negative feedback mechanism. The model provides essential insights into the intricate interplay between legumes and rhizobia, revealing a counteraction where a rhizobal T3SS effector impairs NF signaling by directly targeting NFR5, and NFR1 phosphorylates and inactivates the rhizobal T3SS effector in response.

Results

NopT suppresses the cell death response from overexpression of NFR1 and NFR5

To examine the role of effector proteins in regulating rhizobial infection, *S. fredii* NGR234, a strain with exceptionally broad host–range was chosen. Initial experiments were performed to screen all 15 effector proteins identified from *S. fredii* NGR234 (Kimbrel et

al., 2013), for their ability to suppress or enhance the cell death response in *N. benthamiana* leaves due to co–expression of LjNFR1 and LjNFR5 (Fig. S1A–S1C). Out of the effectors tested, only NopT, a cysteine protease belonging to the YopT family (Shao et al., 2002; Dai et al., 2008), could suppress LjNFR1 and LjNFR5–induced cell death (Fig. 1A and S1D–S1F). Cysteine–93 of NopT is a known residue essential for its protease activity (Dai et al., 2008). In contrast to the wild–type NopT protein, expression of $NopT^{C93S}$, an inactive version, was unable to suppress cell death induced by NFR1 and NFR5 compared with controls (Fig. 1B), indicating the protease activity of NopT is essential for suppression of cell death in *N. benthamiana*. In contrast to the suppressive function on cell death, NopM, an effector protein from *S. fredii* NGR234 reported to have an E3 ligase activity, induced strong cell death when overexpressed in *N. benthamiana* leaves (Fig. 1C).

As controls, we tested whether the action of NopT was specific for NFR1/NFR5 expression or whether it could act generally to suppress cell death. A variety of other proteins have been reported to induce cell death when expressed in *N. benthamiana* leaves; specifically, Avr3a and R3a (Bos et al., 2006), apoptosis regulator BAX (Bcl-2-associated X protein) (Gan et al., 2009), INF1, an elicitor from *Phytophthora infestans* (Vleeshouwers et al., 2006), Arabidopsis AtCERK1 (Cao et al., 2014), and NopM (Fig. 1C). In contrast to the case with LjNFR1 and LjNFR5, expression of NopT was unable to suppress the cell death induced when each of these proteins was expressed in tobacco leaves (Fig. 1D). Hence, the effect of NopT appears to be specific for the NF receptors. These results suggested a hypothesis that rhizobial NopT protease might act directly on the NFR1 and/or NFR5 proteins.

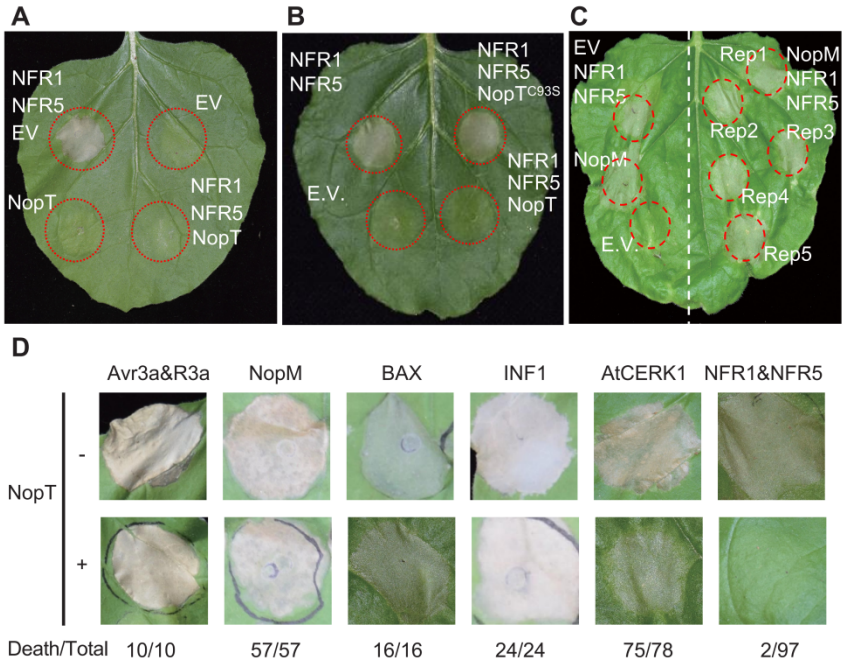

Figure 1. NopT specifically suppresses cell death triggered by NFR1 & NFR5 in *N. benthamiana*. *Agrobacterium* strains harboring genes were NopT or EV infiltrated into *N. benthamiana*,12 hpi followed by infiltration with *agrobacterium* containing NFR1 and NFR5. Different leaf discs indicate where different proteins were expressed. NopT (A) but not NopT^{C93S}, the protease–inactive version of NopT (B) suppressed cell death induced by expression of NFR1 and NFR5. (C) Expression of NopM induced cell death in *N. benthamiana*. (D) Expression of NopT could not suppress the cell death triggered by expression of Avr3a&R3a, NopM, BAX, INF1 or AtCERK1. Digital numbers in (D) represent the number of leaf discs with cell death and total leaf discs tested. All pictures in the Figure are representative of at least three independent biological replicates.

NopT colocalizes with and interacts with NFR1 and NFR5 at the plasma membrane

NopT contains an acylation site that appears to localize NopT to cellular membranes (Dowen et al., 2009). Therefore, we tested the possibility that NopT, NFR1 and NFR5 co–localize on the plasma membrane. *In vivo* bimolecular fluorescence complementation (BiFC) assays were used to examine the colocalization of NopT with LjNFR1 and LjNFR5. NopT, LjNFR1 and LjNFR5 were all C–terminally tagged with nYFP and cYFP. Fluorescence signals representing the associations between NopT and LjNFR1, LjNFR5, as well as itself, were detected at the plasma membrane (Fig. 2A and 2B), suggesting that NopT colocalized with and interacted with both LjNFR1 and LjNFR5. Interactions

between NopT and LjNFR1 and LjNFR5 were further verified using a Split–luciferase (Split–LUC) assay (Fig. 2C). Co–expression of NopT–cLUC and LjNFR1–nLUC or LjNFR5–nLUC produced strong luminescence signals in leaf discs compared with the negative control expressing FLS2–nLUC and NopT–cLUC (Fig. 2C).

It has been known that the acylation of NopT could change its subcellular localization (Dowen et al., 2009). We then exaimed the interaction between NFR1/NFR5 and $NopT^{G50A/C51A/C52A}$, a mutant version on the acylation sites. The interactions between $NopT^{G50A/C51A/C52A}$ and NFR1/NFR5 were significantly reduced compared to $NopT^{WT}$ in Split–LUC assays (Fig. S2A and S2B). While the mutation at catalytic site of NopT ($NopT^{C93S}$) remained similar interaction with NFR1 and NFR5 (Fig. S2C). The interaction results were further confimred by co–immunoprecipitation (co-IP) assay. The C–terminally HA–tagged LjNFR1 and LjNFR5 could be precipitated by anti–FLAG antibody in the sample expressing NopT–FLAG compared with controls (Fig. 2D). The interaction between NopT and LjNFR1 and LjNFR5 suggested that LjNFR5 or LjNFR1 might be a target protein for proteolysis by NopT.

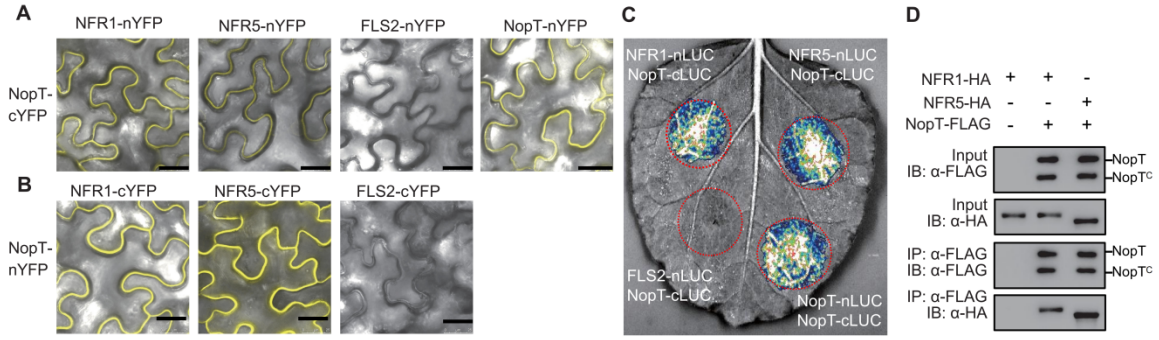

Figure 2. NopT interacts with NFR1 and NFR5. Interactions between NopT and NFR1 and NFR5 were detected using Split–YFP assay (A) and (B), Split–LUC (C) and co–IP (D) assays in *N. benthamiana*. (A) and (B). nYFP and cYFP tags were fused at the C–terminus of NopT, NFR1, NFR5, and negative control FLS2. YFP fluorescence signals represent protein–protein interactions. Scar

bar=25 um. (C). nLUC and cLUC tags were fused at the C–terminus of NopT, NFR1, NFR5, and negative control FLS2. Luminescence signals represent protein–protein interactions. (D). HA–tagged NFR1 and NFR5 and FLAG–tagged NopT were expressed in plant cells followed by immunoprecipitation using anti–FLAG antibody and determined by immunoblot using anti–HA and anti–FLAG antibodies. All data in Figure are representative of three biological replicates.

NopT proteolytically cleaves LjNFR5 at the juxtamembrane domain

A previous study showed that NopT protease activity is detectable upon autocleavage of about 50 amino acids from its N–terminus (Dai et al., 2008). We next tested whether NopT could directly proteolyze LjNFR1 and/or LjNFR5 when co–expressed in *N. benthamiana* leaves. The addition of NopT but not $NopT^{C93S}$, an inactive version, resulted in proteolytic cleavage of LjNFR5–GFP but not LjNFR1–GFP as shown by immunoblotting of the SDS–PAGE gel (Fig. 3A and S3A). The *in vivo* cleavage assay in *L. japonicus* transgenic root also showed that NopT but not $NopT^{C93S}$ resulted in proteolytic cleavage of LjNFR5 (Fig. 3B). Based on the molecular weight change, the cleavage sites were predicted to occur within the cytoplasmic domain (CD) of LjNFR5. Therefore, the CD of NFR5 was constructed as a recombinant protein (Strep–$NFR5^{CD}$–HA) and then co–expressed with NopT–FLAG or the inactive version $NopT^{C93S}$–FLAG in *Escherichia coli* cells. The results showed that the active NopT protease could cleave $NFR5^{CD}$ resulting in a band roughly ~5 kDa less than the control as detected using anti–HA antibody (Fig. 3D). In the same experiment, when the CD of NFR1 was co–expressed with NopT, no cleavage product was detected in immunoblotting assay (Fig. 3C). However, migration of the bands representing NopT or $NopT^{C93S}$ was significantly retarded as seen after immunoblotting (Fig. 3C). This retardation of NopT protein band may be the result of phosphorylation by NFR1.

The cleavage product with ~5 kDa lower molecular weight in the cleavage assay, suggested that the cleavage site is located within the juxtamembrane (JM) position of

NFR5. To test this hypothesis, SUMO–NFR5^{KD}–HA, a recombinant protein with the JM of NFR5 replaced with a SUMO tag, was constructed and used for the cleavage assay. Indeed, NopT could not cleave SUMO–NFR5^{KD}–HA (Fig. S3B). To confirm this conclusion, the JM of NFR5 was used to bridge SUMO and GFP tags to create a recombinant protein, SUMO–JM–GFP. *In vitro* cleavage assay, strong band intensity representing GFP was detected in the flow though sample incubated with NopT but not NopT^{C93S} (Fig. 3E). These data strongly indicated that the cleavage site for NopT is located at the JM of NFR5.

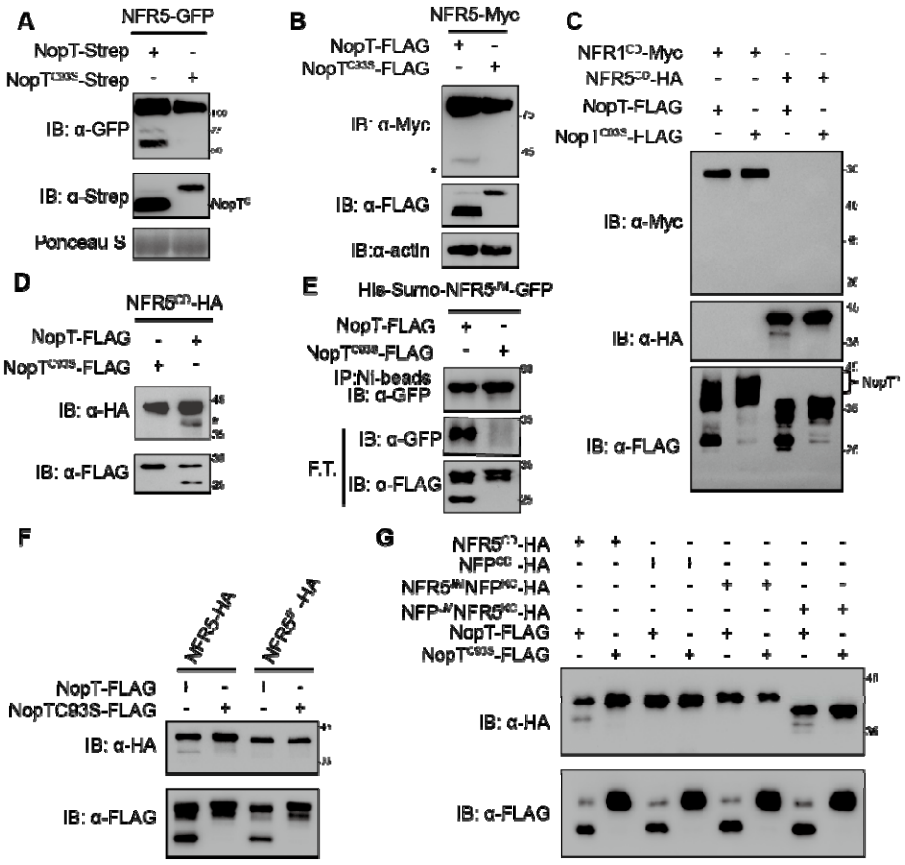

Figure 3. NopT proteolyzes NFR5 at its juxtamembrane domain. (A) NopT but not NopT^{C93S} cleaves NFR5–GFP protein expressed in N. benthamiana cells by releasing NFR5CD–GFP. (B) NopT but not NopT^{C93S} cleaves NFR5-Myc protein expressed in *L. japonicus* transgenic root by releasing NFR5CD-Myc. Asterisk indicated the cleaved variant of NFR5. (C) A repeated experiment testing the cleavage of NFR5^{CD} but not NFR1^{CD} fused with different tags. Asterisk represents the phosphorylated NopT by inducing a band retardation on SDS–PAGE gel. (D) NopT but not NopT^{C93S} cleaves the CD of NFR5 protein expressed in *E. coli* cells by releasing the kinase domain of NFR5. Asterisk indicated the

cleaved variant of NFR5. (E) NopT cleaves a recombinant protein where His–tagged SUMO and GFP is bridged with the JM domain of NFR5. F.T. represents flow through sample after Ni–beads purification. (F) NopT could not cleave a mutant version of NFR5CD–HA with 5 residues in the JM substituted into other residues (S283Y, G294Q, Y303S, A310I, T311Y). (G) NopT could not cleave *Medicago truncatula* NFP and from $NFR5^{JM}$–NFP^{KD}. CD represents cytoplasmic domain, KC represents kinase domain and C-terminal tail region, $NopT^{C}$ indicates the truncated version of NopT after autocleavage by releasing about 50 a.a. at its N–terminus.

The cleavage of LjNFR5 at JM by NopT is dependent on multiple residues of NFR5

NopT has an autocleavage site within its N–terminus, we identified the peptide (DKLLSGV) from Asp–288 to Val–294 of NFR5 (Fig. S4B) as showing the highest similarity with the NopT autocleavage region (DKMGCCA). However, the mutant version of $NFR5^{CD}$ with the peptide (DKLLSGV) replaced with 7 alanines could still be cleaved by NopT (Fig. S3C). NopT and its homlog AvrPphB (Shao et al., 2003b), an effector from the pathogen *Pseudomonas syringa*, belong to the same protein family. Hence, we set up a control experiment by constructing a version of $NFR5^{CD}$, where the "DKLLSGV" motif was replaced with the cleavage sites of AvrPphB. In the cleavage assay, we found that this modified $NFR5^{CD}$ was cleaved by both AvrPphB and NopT, and the cleaved product of modified $NFR5^{CD}$ by AvrPphB shifting faster than by NopT (Fig. S3C), suggesting that the cleavage site of NFR5 by NopT located ahead of "DKLLSGV" motif. As mentioned above, NopT undergoes autocleavage but it is not clear whether this is due to inter–proteolysis or intra–proteolysis. His–205 and Aps–220 of NopT are two other conserved residues required for the protease activity of YopT, another homolog of NopT from *Yesinia* whose function has been extensively studied (Shao et al., 2003b). Therefore, we targeted these residues for site–directed mutagenesis. The cleavage assay showed that NopT could not proteolyze $NopT^{C93S}$, $NopT^{H205A}$, or $NopT^{D220A}$ (Fig. S3D), suggesting that intra–proteolysis might occur and the autocleavage site of NopT could not be used to predict the cleavage site of substrate.

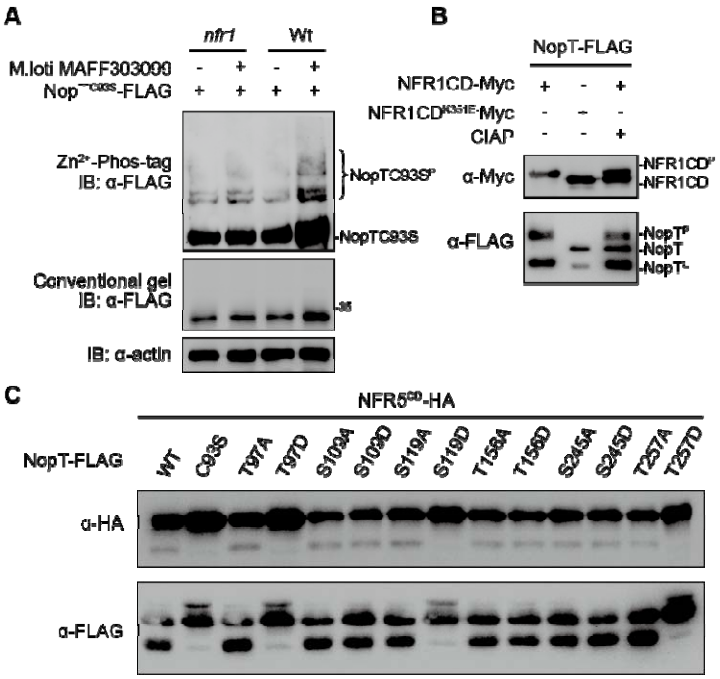

Figure 4. Phosphorylation of NopT by NFR1 suppresses its proteolytic activity. (A) *In vivo* phosphorylation assay in *L. japonicus* roots. Phosphorylation of NopT^{C93S} was induced with rhizobia treatment and dependent on *nfr1*. (B) NFR1^{CD} phosphorylates NopT by inducing a gel band shift determined by immunoblotting. (C) The phoshorylation sites on NopT identified by liquid chromatography–mass spectrometry (LC–MS) were either substituted into alaine (A) or asparatate (D) and subsequently tested for their ability to proteolytically cleave NFR5^{CD}.

To define the cleavage site of NFR5, we created a variety of point mutations covering the JM domain of NFR5 (Val-269 to Cys-320) and first seven a.a. of the kinase domain (Lys-321 to Tyr-327). First, 17 mutant versions of NFR5^{JM} were created with three adjacent amino acids replaced with three alanines for proteolysis assay in *E. coli* cells. However, all 17 mutant versions of NFR5^{CD} could be cleaved by NopT but not NopT^{C93S} (Fig. S3E–S3H). An additional 7 truncated versions of NFR5^{JM}, with deletion of 10 adjacent residues, were created and tested for cleavage by NopT. Surprisingly, the cleavage products were still observed from all 7 truncated versions of NFR5^{JM} (Fig. S3I). The *in vitro* cleavage assay suggested that the JM domain might have multiple sites susceptible to be cleaved by NopT, which is different from the specific cleavage site

identified for its homologous protein AvrPphB. In a parallel experiment, the recombinant protein, His-SUMO-NFR5^{CD}-GST expressed in *E. coli* was subjected for N-terminal protein sequencing determined by Liquid Chromatography Mass Spectrometry analysis after cleavage. Based on allignment using identified peptides, the cleavage site of NFR5 by NopT was mapped to be after four basic amino acids in the JM of NFR5, "RRKK" from 271 to 275 a.a. of NFR5 (Fig. S4C). However, the result is not consistance with the data from cleavage assay. When the region from Tyr-268 to Leu-277 was deleted, NopT could still proteolyze NFR5-CD (Fig. S4I). The cleavage assay suggested that NopT might prefer to proteolyze NFR5 after four polybasic residues in the NFR5^{JM}, but other sites could also be cleaved by NopT.

Because LjNFR5 belongs to a subfamily of plant LYK family proteins that lacks kinase activity (Yang et al., 2022), we then asked whether NopT could proteolyze other LYK proteins in this subfamily, which might be helpful to characterize the biochemical function of NopT. Hence, the CDs from Arabidopsis AtLYK5, *L. japonicus* LjLYS11 and *M. truncatula* MtNFP were used for cleavage assays in the presence of NopT. As shown in Fig. S3J, NopT, but not NopT^{C93S}, could cleave the CDs of both AtLYK5 and LjLYS11. Replacement of NFR5^{JM} with the JM domains from either AtLYK5 or LjLYS11 also resulted in cleavage by NopT (Fig. S3J). The data strongly indicated that NopT could cleave both AtLYK5 and LjLYS11 at their JM domains. Based on sequence analysis of the JM region of NFR5 and its homologous proteins, five conserved residues (Ser-283, Gly-294, Tyr-303, Ala-310, Thr-311) were identified and mutated for the proteolysis assay (Fig. S4B). As shown in Fig. 3F, the mutant version of NFR5 (i.e., NFR5^{CD} with five amino acid mutations) could not be cleaved by NopT. Interestingly, NopT coud not protelyze MtNFP^{CD} (Fig. 3G). Then, we generated two recombinant proteins, by switching the JM between NFR5^{CD} and NFP^{CD}, generating NFR5^{JM}-NFP^{KC} (KC represents kinase domain and C-terminal tail region) and NFP^{JM}-NFR5^{KC} for *in vitro* cleavage assays. As

shown in Fig. 3G, NopT could proteolyze NFP^{JM}-$NFR5^{KC}$ but not $NFR5^{JM}$-NFP^{KC}. The data suggested that the cleavage of NFR5 by NopT might be dependent on the confirmational structure of $NFR5^{KC}$ and/or other specific amino acids in $NFR5^{KC}$. To define this, two additional recombinant proteins with large switch between $NFR5^{CD}$ and NFP^{CD}, $NFR5^{268-445}$-$NFP^{458-595}$ and $NFP^{270-457}$-$NFR5^{456-595}$, were constructed for proteolysis (Fig. S3K). However, both of them could be cleaved by NopT, suggesting that a much large region on $NFR5^{KC}$ is required for being proteolyzed by NopT. Based on all these cleavge results, we concluded that NopT could proteolyze NFR5 at the JM domain, which nonadjacent mutiple residues within the $NFR5^{JM}$ and the specific KC region are required for the proteolysis.

NopT phosphorylation by LjNFR1 suppresses its proteolytic activity

The perception of rhizobia NFs by the heterocomplex of NFR1 and NFR5 involves the trans–phosphorylation from the NFR1 kinase to the pseudo–kinase NFR5 (Madsen et al., 2011). Rhizobial effector NopT associates with both NFR1 and NFR5, which suggests that NopT might be a phosphorylation target of NFR1 and involved in the transphosphorylation process between the two receptors. Kinase assays showed that NFR1–CD but not the kinase–inactive $NFR1^{K351E}$–CD (Lys-351 is the conserved residue required for ATP binding) could phosphorylate NopT (Fig. 3C and 4B) and NFR5–CD (Fig. S5) as shown by band retardation on SDS–PAGE gels identified using immunoblotting. The band representing phosphorylated NopT shifted upon the addition of a commercial phosphatase, calf intestinal alkaline phosphatase (Fig. 4B), indicating that NopT as well $NFR5^{CD}$ are phosphorylation targets of the NFR1 kinase. NopT autocleavage also gives two bands and the site mutant of NopT at C93S did not affect the interactions between NFRs(Fig. S2C). To avoid multi-bands interference of cleaved NopT, $NopT^{C93S}$ was expressed in both wild type plants and *nfr1* mutant then treated with rhizobia or water. After analyzed by

Zn^{2+}-Phos-tag PAGE gel, several shifted bands were strengthened after rhizobia treatment in WT roots but not in the *nfr1* mutant roots (Fig. 4A), suggesting that the phosphorylation of NopT could be induced by NFR1 and multi-sites of NopT were phosphorylated *in planta*. The phosphorylation sites of NopT were further identified using Liquid Chromatography Mass Spectrometry (Table S1). We then addressed whether NopT phosphorylation by NFR1 regulates its proteolytic activity on NFR5. All the potential phosphorylation sites of NopT were substituted into either alanine in order to block phosphorylation of these sites or aspartate, which mimicks the acidic condition representing a phosphorylated status. These mutant proteins were then used in the cleavage assay. Aspartate substitutions on three phosphorylation sites of NopT, Thr–97, Ser–119, and Thr–257, resulted in the loss of the ability of NopT to cleave NFR5–CD, as well as the ability to autocleave (Fig. 4C). In contrast, NopT proteins with alanine substitutions on these three sites retained the ability to cleave NFR5–CD and to autocleave (Fig. 4C). The data suggest that phosphorylation of NopT by NFR1 likely inhibits proteolytic activity, retaining a fully functional NFR5 and a full length NopT.

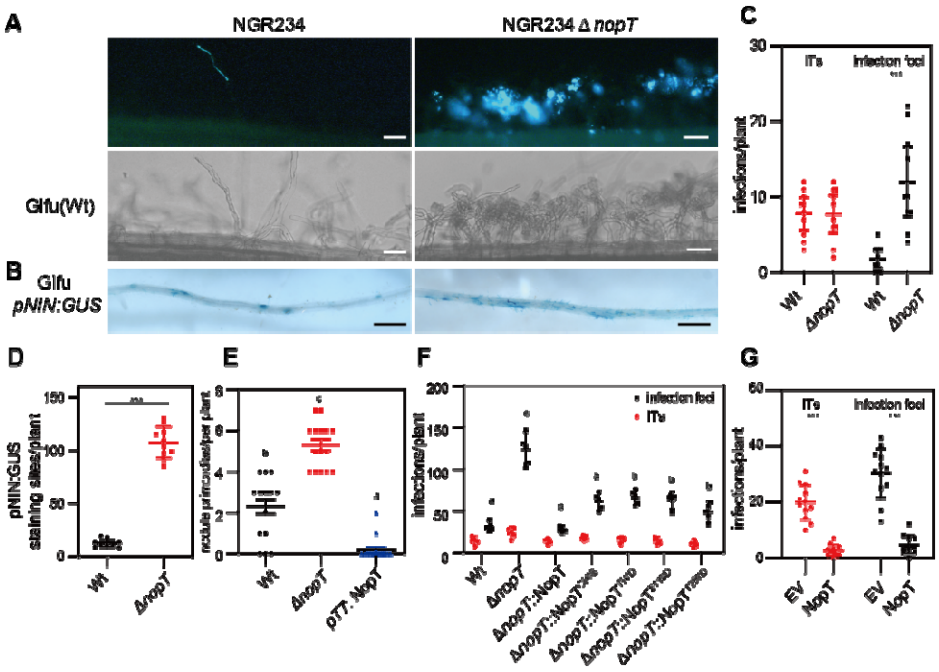

Figure 5. NopT regulates rhizobial infection in *L. japonicus*. (A) Rhizobial infection in *L. japonicus* using GFP-labelled WT and *nopt* mutant strains of *S. fredii* NGR234. Fluorescent, GFP-expressing

bacteria are imaged in Cyan. Scar bars=12.5μm. (B) GUS staining pictures from the roots of *L. japonicus* transgenically expressing GUS under *p*NIN promoter inoculated with WT and *nopT* mutant strains of NGR234. Scar bars=1mm (C) Statistical analysis of rhizobial infection in A (n=10, Student's *t*–test: P < 0.01). (D) Statistical analysis of GUS straining sites in B (n=10, Student's *t*–test: P < 0.01). (E) Nodule primordia number on the roots 14dpi after inoculation WT, *nopT* mutant strains or *pT7*: NopT (n=16, Student's *t*–test: P < 0.01). (F) Infection foci number from the wild type plant roots inoculated with WT strains and *nopt* mutant strains expressing NopT with different variations (n=5, Student's *t*–test: P < 0.01). (G) Statistical analysis of rhizobial infection in *L. japonicus* transgenic root expressing GFP (EV, empty vector control) or NopT using DsRed-labeled *M. loti* MAFF303099 (n=8, Student's t–test: P < 0.01).

NopT dampens rhizobial infection

The fact that *S. fredii* NGR234 NopT could directly target and cleave NFR5 indicates that NopT may be an important player regulating rhizobial infection in legumes. Nod factor signal is known to function in the early stage of rhizobial infection and nodulation specificity (Geurts et al., 2005; Wang et al., 2012). Prior work showed that type three secretion system of *S. fredii* NGR234 might not regulate nodule numbers few weeks after inoculation in *L. japonicus* (Ausmees et al., 2004). Therefore, we focused on the early stage of rhizobial infection. Indeed, inoculation with GFP–labelled *S. fredii* NGR234Δ*nopT* induced a massive infection within the root hairs of *L. japonicus* (Gifu) plants compared with the favorable infection by the NGR234 wild type strain (Fig. 5A and 5C). Transgenic expression of NopT in *L. japonicus* root hair reduced the infection of *Mesorhizobium loti* MAFF303099 (Fig. 5G). In *L. japonicus* plants transgenically expressing *pNIN*:*GUS*, greater range of GUS expression (Fig. 5B and 5D) and formation of more nodule primordia (Fig. 5E) also reflected a stronger plant response to infection by NGR234Δ*nopT* relative to the wild–type strain. To confirm the massive infection is due to the loss of NopT, NopT was expressed in the *S. fredii* NGR234Δ*nopT* strain and used for inoculation in *L. japonicus*. Complementation with NopT in NGR234Δ*nopT* reduced the massive infection foci to the similar levels as the WT strain (Fig. 5F). We then tested whether the proteolytic activity of NopT is required for rhizobial infection. The

protease–dead version of NopT^{C93S} and three phosphorylation mimic versions of NopT, i.e., NopT^{T97D}, NopT^{S119D}, and NopT^{T257D}, which lack proteolytic activity, were individually expressed in NGR234Δ*nopT*. Compared with the high levels of infection foci induced by NGR234Δ*nopT* in *L. japonicus* plants, inoculation with these four mutant strains induced much lower levels of infection, albeit slightly higher than that induced by the wild–type strain (Fig. 5F). Inoculation with NGR234Δ*nopT* produced more nodule primordia, while over-expression of NopT under the control of T7 promoter in *S. fredii* NGR234 WT strain reduced the numer of nodule primordia, compared with wild–type strain inoculation 14 dpi (Fig. 5E). To verify whether the cleavage of NFR5 reduce rhizobial infection, NFR5–WT and NFR5^{5m}, a mutant version with 5 amino acids substitutions at JM that is resistant to NopT cleavage, were expressed in the *nfr5-3* roots under the control of its native promoter. However, expression of NFR5^{5m} was not observed to rescue the infection phenotype of *nfr5-3* mutant plants (Fig. S5A). The possible reason is that amino acids substitutions at JM might lead to a conformation change of NFR5 that is required for its function in symbiotic signaling transduction. Therefore, NFR5-NFP^{KC}, the KC domain of NFR5 replaced with KC domain of NFP, was expressed in the roots under the control of native promoter (Fig. S5B). In the *nfr5-3* roots expressing NFR5-NFP^{KC}, no difference of rhizobial infection was observed between *S. fredii* NGR234Δ*nopT* and *S. fredii* NGR234 wild type strain, suggesting that the cleavage of NFR5 reduced the rhizobial infection levels. All these data strongly indicated that the protease activity of NopT, the phosphorylation status of NopT, and the proteolysis of NFR5 are important for rhizobial infection.

The truncated version NopT$^{\Delta N50}$ cleaves NFR5 but fails to interact with NFR1

The significance of rhizobial NopT in mediating rhizobial infection led us to analyze its homologs from other rhizobium species. Sequence comparisons based on the amino acids

of NopT homologs showed that *Sinorhizobium* and *Bradyrhizobium* were located in different clades (Fig. S7). *B. diazoefficiens* (USDA110) is a typical *Bradyrhizobium* strain used to study the symbiotic interaction with soybean. Two NopT homologous genes, named $NopT1_{USDA110}$ and $NopT2_{USDA110}$ were identified from the USDA110 genome (Fotiadis et al., 2012). However, when tested, neither $NopT1_{USDA110}$ or $NopT2_{USDA110}$ could not cleave NFR5 compared to $NopT_{NGR234}$ (Fig. 6A). The possible scenario is that NopT homologs from *Bradyrhizbium* species might have lost the ability to cleave NFR5 and/or may act on other, unknown cellular target proteins. The genome of some *Sinorhizobium* species, for example *S. fredii* USDA257 and S. *fredii* HH103, encode *NopT* homologous genes predicted to produce same truncated proteins with a 57 aa deletion from its N–terminus, relative to the NGR234 NopT sequence, which is almost the same as the truncated $NopT_{NGR234}$ after autocleaveage. When these NopT homologs (i.e., $NopT_{USDA257}$ and $NopT_{HH103}$) were tested, both were observed to have the ability to cleave NFR5 (Fig. 6A). However, these NopT homologs could not suppress the cell death triggered by NFR1 and NFR5 in *N. benthamiana* leaves (Fig. 6B) and failed to complement the massive infection of NGR234Δ*nopT* (Fig. 6C and 6D), suggesting that $NopT_{USDA257}$ and $NopT_{HH103}$ retained the same catalytic activity as $NopT_{NGR234}$ but might have different substrates. We then asked whether the truncated version of $NopT^{\Delta N50}$, which mimics the truncated NopT after autocleavage, retained the ability to interact with NFR1. However, after repeated tests, the direct interaction between $NopT^{\Delta N50}$ and NFR5 could be detected but not the corresponding interaction with NFR1 using Split–LUC assays (Fig. S2D). The data suggest that some *Sinorhizobium* species, for example, *S. fredii* NGR234, *S. fredii* USDA257 and *S. fredii* HH103, use a truncated NopT to regulate the rhizobial infection process in a way that avoids negative regulation by NFR1 phosphorylation, which is not true of all rhizobial strains that possess NopT homologs.

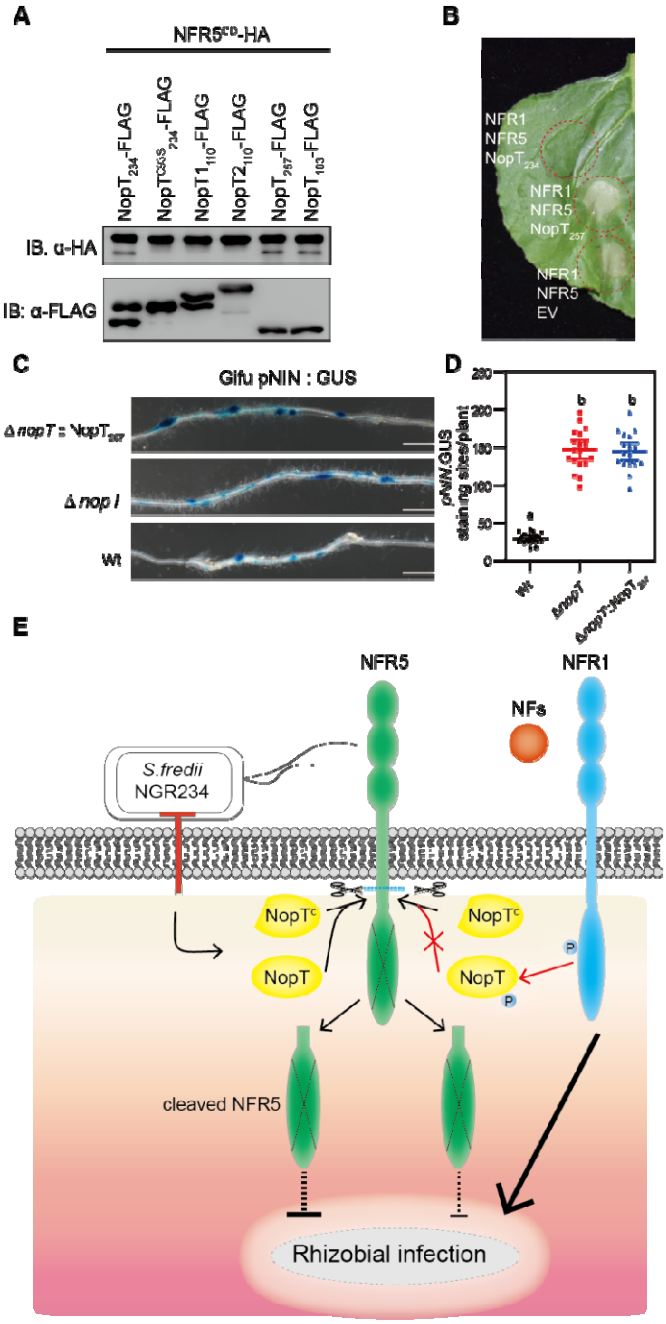

Figure 6. Working model of NopT in association with NF receptors. (A) $NopT_{234}$, NopT from *S. fredii* NGR234; $NopT1_{110}$ and $NopT2_{110}$, NopT homologs from *B. diazoefficiens* USDA110; $NopT_{257}$, NopT from *S. fredii* USDA257; $NopT_{103}$, NopT from *S. fredii* HH103. All NopT homologs were tested in the proteolysis assay using $NFR5^{CD}$ as a target. (B) Rhizobial infection $NopT_{257}$ could not inhibit the cell death triggered by NFR1 and NFR5 in *N. benthamiana*. (C)The indicated rhizobial strains induced *nin::gus* expressing in *Lotus* root. Scar bars=2.5mm. (D) Statistical analysis of GUS straining in C (n=19, Student's *t*–test: $P < 0.01$). (E) A proposed model of NopT in association with NF receptors. Both NopT and $NopT^{C}$ after autocleavage exert proteolytic activities to cleave NFR5 at the

juxtamembrane domain to release the kinase domain of NFR5 (cleaved NFR5). NFR1 phosphorylates intact NopT, but not $NopT^{C}$, to block its proteinase activity.

Discussion

Plant-microbe interactions involve two sophisticated and intelligent organisms, each employing distinct "weapons" or strategies to communicate mutually, thereby securing more nutrients for their survival (Jones and Dangl, 2006; Schubert et al., 2020). A well-established regulatory model arises from the study of plant-pathogen interactions, where T3SS effectors from gram-negative bacteria are injected into plant cells to directly target and suppress the plant's immune pathway, favoring pathogenic bacterium infection (Jones and Dangl, 2006). However, the unique model of mutual regulation between legumes and rhizobia in symbiotic interactions remains largely unknown. The broad goal of this study was to offer essential insights into the mutual regulation mechanisms whereby rhizobial effectors directly target symbiotic signaling pathways to dampen their infection in host cells.

Understanding how plants recognize different microbes as "friends" or "foes" is a central question in biology. As the first line of plant response to microbes, the perception of microbial signals by receptor proteins from plants is essential for inducing different signaling pathways to establish various interaction patterns–either symbiotic, pathogenic, or no responses (Zipfel and Oldroyd, 2017). Therefore, it is not surprising to discover that the direct targeting of these receptors by bacterial effectors represents an efficient strategy to manipulate plant signaling pathways for enhancing bacterium infection. In the well-studied *Arabidopsis–Pseudomonas syringa* interaction model, the flagellin receptor FLS2 (Flagellin Sensing 2) and its coreceptor BAK1 (BRI1-[Brassinosteroid insensitive

1]-associated receptor kinase 1), triggering plant immunity against pathogenic infection, are targeted by several effectors from bacteria (Zipfel et al., 2004; Sun et al., 2013). For example, AvrPto and HopB1 could suppress the kinase activity and cleave the Arabidopsis receptor complex, respectively (Xiang et al., 2008; Li et al., 2016). AvrPtoB, an E3 ligase in *P. syringae*, targets FLS2 to promote its degradation, resulting in decreased immune responses in plant cells (Goehre et al., 2008). Considering the evolutionary importance of effectors in infection, it is rational to identify that the rhizobial effector NopT, a member of the C58 protease family, can directly target NFRs, manipulating symbiotic signaling pathways in plants. This was demonstrated using a unique screening system in *N. benthamiana* leaves (Fig. S1A-C), in which co-expression of two symbiotic receptors, NFR1 and NFR5, could lead to plant cell death to identify NopT, the only effector from *S. fredii* NGR234. *S. fredii NGR234*Δ*nopt* mutant strains hyperinfect *L. japonicus* roots, and overexpression of NopT in the roots reduces rhizobial infection (Fig. 5A-5D), consistent with the observed suppression of cell death in *N. benthamiana* leaves (Fig.1A). The interaction between NopT and NFRs has been verified and is impaired by the acylation site of NopT (Fig.2 and S2A), suggesting that the plasma membrane localization of NopT is essential for targeting NFRs.

In the extensively studied context of microbial pathogenesis, various effectors from pathogens have been proposed to directly suppress the immune system and promote virulence in host cells (Tang et al., 2017; Schubert et al., 2020). The C58 protease family, including YopT and AvrPphB, represents such effectors that disarm the host defense system to favor pathogenic infection in both animals and plants (Shao et al., 2003a; Zhang et al., 2010). *Yersinia* YopT cleaves the Rho family GTPase to disrupt the actin cytoskeleton, inhibiting the phagocytosis of pathogens by hosts (Shao et al., 2003a). Conversely, *P. syringae* AvrPphB

cleaves multiple members of the RLCK (receptor-like cytoplasmic kinase) subfamily VII to suppress the PTI response (Zhang et al., 2010). In contrast, the cleavage of PBS1 functions as a "decoy" to trigger strong immunity against bacterial infection (Shao et al., 2003b). We confirmed that NopT cleaves NFR5 at the JM domain through different assays (Fig.3). Mutants with five dispersed residues (S283, G294, Y303, A310, T311) at the JM domain (Fig.3F) and the replacement of $NFR5^{KD\text{-}CT}$ with $NFP^{KD\text{-}CT}$ (Fig.3G) resist cleavage by NopT, suggesting a joint decision of cleavage involving both the JM domain and KD-CT domain. Although belonging to the same protease family, the cleavage sites of NopT and YopT are polybasic (Shao et al., 2003a; Schmidt, 2011), in contrast to AvrPphB, whose cleavage site is canonical with seven adjacent amino acids involved (Kim et al., 2016). The different cleavage sites of YopT-type effectors indicate that bacteria regulate different physiological pathways to establish specific interactions with host plants.

Similar to the plant pathogenic effector AvrPphB, the protease activity of NopT appears to be conserved for this function by cleaving the soybean PBS1 homolog protein to restrict symbiosis (Khan et al., 2022). Indeed, transient expression of *S. fredii* NopT in *A. thaliana* and *N. tabacum* could induce strong immune responses and hypersensitive cell death (Fig. S8), indicating that rhizobial NopT might act as an avirulent effector in some nonhost plant species. Interestingly, we failed to obtain stable transgenic lines constitutively expressing NopT in *L. japonicus*. However, the generation of transgenic root hairs was not affected, implying that NopT might act as an Avr effector whose overexpression leads to whole plant lethality but not root growth. Therefore, given this conservation of protease function, it is consistent with a successful Avr effector that NopT has the ability to proteolyze not only NFR5 but also Arabidopsis AtLYK5 and *L. japonicus* LjLYS11,

two receptors with chitin-binding affinities that mediate plant PTI responses (Cao et al., 2014; Gysel et al., 2021). NFR5, AtLYK5, and LjLYS11 are LYKs belonging to the same subfamily that lacks kinase activities. Thus, NopT may not only suppress the nod factor–mediated symbiotic signal to avoid excessive infection by *S. fredii* NGR234 but also function in inhibiting the signal triggered by chitin-like compounds. The cleavage of receptor-like kinases (RLKs) may be an overlooked strategy to regulate their function in plant biology compared to the well-studied phosphorylation to control RLK activation. While cleavage regulation is well studied in neurobiology, e.g., the Notch signal, the proteolysis of each Notch molelue leads to signaling activation (Kopan and Ilagan, 2009). Arabidopsis BAK1, identified as an universal co-receptor to regulate plant growth and MAMPs perception, undergoes proteolytic cleavage, which is important for both BR signaling and PTI response with an unclear mechanism (Zhou et al., 2019). NFR5 is a pseudokinase that functions as an output of NF signaling. The cleavage of NFR5 by rhizobial NopT releases the cytoplasmic domain of NFR5, but the precise function of whom is of interest to be determined.

The legume–rhizobial symbiosis is a unique case in the context of plant–microbe interactions. Mutual regulation between pathogenic effectors and host proteins has been reported in plant pathogenesis. For example, the *Pseudomonas* conserved effector AvrPtoB could directly target key components in the immunity pathway to promote its virulence (Goehre et al., 2008). However, the virulent function of AvrPtoB could either be enhanced or dampened by host proteins. AvrPtoB could be phosphorylated by SnRK2.8 to promote its virulence activity (Lei et al., 2020). Plant lectin receptor-like kinase LexRK-IX.2, Pto, and Fen kinases could also phosphorylate AvrPtoB to inactivate its E3 ligase activity and undermine its ability to suppress PTI (Ntoukakis et al., 2009; Xu et al., 2020). A similar

strategy was used by legumes to dampen the "virulence" of the rhizobial effector NopT, favoring mutualistic infection. NFR1 phosphorylates NopT at several residues. The phosphomimetic NopTs (i.e., $NopT^{T97D}$, $NopT^{S119D}$, and $NopT^{T257D}$) are unable to cleave itself and NFR5 (Fig. 4C). The expression of these phosphomimetic NopTs separately in *S. fredii* NGR234Δnopt mutant strains cannot complement the hyperinfection phenotype (Fig.5F). These data indicate that *L. japonicus* deploys NFR1 to phosphorylate NopT to dampen its catalytic activity and may protect NFR5 from cleavage, favoring rhizobial infections. However, $NopT^{\Delta N50}$, mimic version of autocleaved NopT, retained the ability to interact with NFR5 but not NFR1 (Fig. S2D). Moreover, intact NopT, but not autocleaved NopT, are migrated by expressing $NFR1^{CD}$ in immunoblotting (Fig. 3C and 4B), suggesting autocleaved NopT may escape from being phosphorylated and inactivated by NFR1.

In different rhizobium species, a variety of NopT homologs were characterized. NopT homologs from some *Bradyrhizobium* species lose the ability to cleave NFR5, while NopT homologs from some *Sinorhizobium*, truncated versions without about 50 a.a. at its N-terminus, retain the ability to cleave NFR5 (Fig. 6A). The type three secretion signal depends on the N-terminal of effectors (Akeda and Galán, 2005). However, an earlier study has shown that NopT from *S. fredii* HH103 exhibited a positive effector on nodulation in soybean SN14 cultivar (Li et al., 2023), suggesting that another unknown mechanism might be involved in $NopT_{HH103}$ secretion. Interestingly, these truncated NopTs still keep the function to cleave NFR5 (Fig. 6A) and autocleaved $NopT_{NGR234}$ cannot interact with NFR1 (Fig. S2D), indicating that NopTs from those strains and autocleaved $NopT_{NGR234}$ might lose the ability to be suppressed by NFR1. Notably, natural truncated NopT from *S. fredii* USDA257 and *S. fredii* HH103 are the same in protein sequence, but

they lack the acylation site compared with $NopT_{NGR234}$. Therefore, $NopT_{USDA257}$ and $NopT_{HH103}$ lose the ability to suppress cell death triggered by NFR1 and NFR5 in *N. benthamiana* leaves (Fig. 6B) and failed to complement the massive infection of NGR234*ΔnopT* (Fig. 6C and 6D), implying $NopT_{USDA257}$ and $NopT_{HH103}$ may have a different target from $NopT_{NGR234}$ in the host plant. In addition, knockout of NopT in *Bradyrhizobium* sp. ORS3257 was shown to result in uninfected nodule formation, suggesting that, in this system, $NopT_{ORS3257}$ might play a role in nodule formation (Teulet et al., 2019). The versatile function of NopT homologs in different rhizobium species suggests that different regulatory processes might be involved in specific rhizobial symbiosis.

In this study, we present a mutual regulation model in which the rhizobial effector NopT directly targets NFR5 to suppress symbiosis signals and is then inactivated by NFR1 *via* phosphorylation. NopT appears to retain some pathogenic-like features in that it can cleave the *Arabidopsis* chitin receptor AtLYK5 and induce cell death in some non-leguminous plants, such as *N. tabacum* and *Arabidopsis*. Thus, the cleavage of NFR5 by NopT might be due to the structure similarity to AtLYK5 targeted by NopT. The suppression of proteolytic activity of NopT *via* phosphorylation by NFR1 appears to work as a feedback loop to allow symbiotic signaling in compatible hosts. The model (Fig. 6E) provides essential insights into the legume–rhizobial symbiosis, where rhizobia deploy an effector to dampen symbiotic signaling, and legumes slightly recur infection by suppressing NopT to employthe nod factor signal in response. Even though this couple, legume and rhizobia, tries to get together and strives to improve their living conditions, we catch a glimpse into the arguments and the recovery conversations between them.

Materials and Methods

Plant materials

Lotus japonicus Gifu B–129 cultivar was provided by the Center for Carbohydrate Recognition and Signaling (https://lotus.au.dk/), and used as wild type for nodulation assays. The Gifu *pNIN*:*GUS* transgenic line was kindly provided by Dr. J. Stougaard from the Aarhus University (Heckmann et al., 2011). All *L. japonicus* seeds were treated with concentrated sulfuric acid for 10 min, followed by surface sterilization in 1% (w/v) NaClO for 8 min. After synchronization of germination at 4°C in the dark for 2 d, the seeds were placed on half–strength Murashige & Skoog (MS) medium containing 0.8% (w/v) agar for germination at 22°C for 2 d in the dark. Seedlings were then transferred to growth pots containing vermiculite supplied with half–strength B&D (Broughton & Dilworth) medium without nitrogen under long–day conditions (16–h light/8–h dark) at 22°C. Ten–day–old seedlings were inoculated with *Sinorhizobium fredii* NGR234 (OD_{600}=0.02) for infection assays.

Plasmid construction

All plasmids used in this study were generated using MultiF Seamless Assembly Mix (ABclonal, catalog number RK21020). The plasmid pGWB514 was used as an original plasmid for all binary vector construction (Nakagawa et al., 2007). Briefly, Different tags including HA tag, Myc tag, FLAG tag, Strep tag, nLUC, cLUC, and GFP were respectively amplified using a forward primer containing a *Kpn*I site and ligated into pGWB514 digested with *Xba*I and *Sac*I using seamless cloning method as described above. The generated plasmids were named pG5XX–HA, pG5XX–Myc, pG5XX–FLAG, pG5XX–nLUC, pG5XX–cLUC, pG5XX–GFP, respectively. The coding sequences of *L. japonicus NFR1* and *NFR5* were cloned into pGWB514 and pG517 between *Xba*I/*Kpn*I to generate NFR1–HA and NFR5–Myc fusion constructs under the control of the 35S promoter. then, the DNA fragment containing *pro35S*:NFR5–Myc–NosT was amplified and cloned into pG514–NFR1 at *Sbf*I. The final plasmids contained

pro35S:NFR1–HA–NosT and *pro35S*:NFR5–Myc–NosT. Rhizobial genes encoding effectors from *S. fredii* NGR234 were cloned into pG5xx–FLAG between *Xba*I/*Kpn*I. To detect the interaction between NFR1/NFR5 and NopT in *N. benthamiana*, the full–length *NFR1/NFR5*, *NopT* and *AtFLS2* coding sequences were cloned into pG5xx–Nluc, pG5xx–Nluc, pSPYCE(MR) and pSPYNE(R)173 (Waadt et al., 2008). For cleavage assay in *N. benthamiana*, the *NFR5* and *NopT* coding sequences were cloned into pG5XX–FLAG GFP and pG5xx–Strep respectively. For cleavage assay in *E. coli*, the sequence encoding the cytoplasmic domain of NFR5 was cloned into pACYC duet Strep–HA, the sequences encoding the kinase domain of NFR5 fused to HA tag and the juxtamembrane domain of NFR5 fused to the GFP tag was cloned into pSUMO. The point mutants in $NFR5^{CD}$ and NopT were created from the pACYC duet Strep–$NFR5^{CD}$–HA and pET28a NopT–FLAG template using site–directed mutagenesis PCR. For *in vivo* cleavage assay in *L. japonicus*, NopT-FLAG or $NopT^{C93S}$-FLAG was cloned into pUB GFP between *Xba*I and *Kpn*I, and then 35S-NFR5-Myc-NosT was cloned in pUB NopT GFP at *Pst*I. For phosphorylation assay, the sequence encoding the cytoplasmic domain of NFR1 fused to a Myc tag was cloned into pCDF duet. For rhizobium infection assays, 300 bp upstream of *NopT* and site mutants of *NopT* were fused by overlapping PCR and cloned into pHC60.

Transient expressing and in *Nicotiana* species

The plasmids for transient expression of INF1, Avr3 and R3a in *N. benthamiana* were kindly gifted by Dr. Juan Du from HZAU. *Agrobacterium* (*Agrobacterium tumefaciens*) strain EHA105 carrying various constructs were mixed with an *Agrobacterium* culture harboring the P19 suppressor in an infiltration buffer (10 mM $MgCl_2$, 10 mM MES–KOH pH 5.8 and 200 μM acetosyringone). After incubating 2 h at room temperature, *Agrobacterium* cultures were infiltrated into the leaves of 4–week–old *N. benthamiana* and *N. tabacum*. Leaves were harvested for analysis at two days post infiltration. The cell death suppression assay in *N. benthamiana* was performed as described previously (Wang et al., 2011).

Hairy Root Transformation in *Lotus japonicus*

The hairy root transformation assays were performed as described previously(Li et al., 2018). In brief, surface-sterilized seeds were germinated and grown in the MS plate without sucrose (23°C dark for first 3 days and 23°C 16 h light/8 h dark for next two days). Then seeds were cut at the middle of the hypocotyl and co-cultivation with *A. rhizogenes* carry pUB GFP and pUB NopT-FLAG GFP respectively (23°C dark for first 3 day and 23°C 16 h light/8 h dark for next 2 day). Transfer the plants onto B5 media. After about 15 days, the plants were picked up for further analysis by cutting the root without expressing florescent proteins. For rhizobial infection assays, data were collected at 9dpi for *S.fredii* NGR234 and 6dpi for MAFF303099

NFR5 cytoplasmic domain cleavage assay

For cleavage assay in *E. coli*, Strep–NFR5^{CD}–HA or Strep–NFR5^{CD}–HA were co–expressed with NopT–FLAG or NopT^{C93S}–FLAG by using Duet expressing vectors (Novagen) (Han et al., 2017). Bacterial cell cultures were treated with 0.5 mM IPTG at 22°C for 15 h. The bacterial pellet was resuspended in extraction buffer consisting of Tris–HCl (pH 7.3), 150 mM NaCl, 5 mM EDTA, 0.5% (w/v) SDS and 0.5% (v/v) Triton X–100. After adding SDS loading buffer and boiling at 100°C for 5 min, total proteins were detected with anti–HA–peroxidase (Sigma, clone 3F10), anti–FLAG (Sigma, F1804), and anti–Strep (ABclonal, AB_2863792) antibodies.

For *in vitro* cleavage assays, Sumo–NFR5^{JM}–GFP and NopT–FLAG recombinant proteins were purified, and 3 μg NopT–FLAG and 1 μg Sumo–NFR5^{JM}–GFP were incubated in a test tube at 22°C for 7 h. The cleavage products were detected with anti–GFP antibody by immunoblot (ABclonal, AB_2770402).

For in vivo cleavage assays, the transgenic root was collected at about 15 days after induction of hairy roots. 2% protease inhibitors (Sigma, P9599) were added in extraction buffer. The actin proteins were detected with anti-Actin antibody (ABclonal, AC009).

Phosphorylation assays

For phosphorylation assays in *E. coli*, His–NFR1^{CD}–Myc or His–NFR1$^{CD–K351E}$–Myc and NopT–FLAG–His were co–expressed by using Duet expressing vectors (Novagen) with 0.5 mM IPTG at 28°C for 18 h. After purifying NFR1^{CD} and NopT at the same time, CIAP (TaKaRa, 2250B) was added and incubated at 37°C for 3 h. The mobility shift of NFR1^{CD} and NopT was detected with anti–Myc (Bio–Legend, 626808) and anti–FLAG (Sigma, F1804) antibodies by immunoblot analysis.

For phosphorylation assays in *L. Japonicus* roots, NopT^{C93S}-FLAG was expressed in the *nfr1* mutant and wild type plants, respectively. Transfer the plant with florescent root to half–strength B&D media for 5 days. After treat with water and rhizobia respectively, the total proteins were drawn by extraction buffer with addition 2% protease inhibitors cocktail (Sigma, P9599) and 2% phosphatase inhibitors cocktail (Yeasen,20109-A), then followed with TCA precipitation to remove various contaminants (e.g. EDTA, surfactant). Phosphorylation of NopT^{C93S} proteins was analyzed by 50μM Zn^{2+}-Phos-tag SDS-PAGE and detected with anti–FLAG (Sigma, F1804) antibodies by immunoblot analysis.

BiFC and Split–LUC assays in *N. benthamiana*

In BiFC assay, the eYFP fluorescence of fusion proteins was assayed 2–3 days after infiltration using a confocal microscope (Leica TCS SP8). For the Split–LUC assay, *N. benthamiana* leaves were collected at 2 dpi sprayed with a solution of 1 mM D–luciferin (Promega, E1603) and 0.02% (v/v) Triton X–100. After a dark–adaptation of 5 min, bioluminescence images were acquired using a Tanon Bio–Imaging System (Tanon, Shanghai, 4600).

Liquid chromatography mass spectrometry

For proteomics analysis of NopT phosphorylation sites, *NopT* and *NFR1–CD* or *NFR1–CD*^{K351E} were co–expressed in *E. coli*, then proteins were purified using Ni–Charged Resin (GenScript, Cat. No. L00223). The bands of NopT^{P} and NopT, as control, were cut and destained by 50 mM triethylammonium bicarbonate (TEAB) and 50% (v/v) acetonitrile (ACN) in 50 mM TEAB followed by washing with 100% ACN until the gel turned white. The protein bands were then in–gel digested with sequencing–grade trypsin. LC–MS analysis was performed by Novogene Co., Ltd. (Beijing, China).

For identificaiton of the cleavage site on NFR5, NopT and the recombinant protein, His-Sumo-NFR5-GST, were co-expressed in *E. coli* followed by protein purification using Glutathione Resin (GenScript, Cat. No. L00206). About 80μg cleaved NFR5 was collected for analysis. The protein bands were digested with trypsin,glu-C, chymotrypsin and pepsin. LC–MS analysis was performed by Oulu Biotechnology Co., Ltd. (Shanghai, China).

Supplemental data

Supplemental Figure 1. Analyses of the functions of all 15 effectors from *S. fredii* NGR234 in preventing LjNFR1- and LjNFR5-induced cell death in *N. benthamiana* leaves. Supplemental Fig. 2. Split–LUC assay testing the interactions between different NopT mutant and NFRs.

Supplemental Figure 2. Split–LUC assay testing the interactions between different NopT mutants and NFRs.

Supplemental Figure 3. NopT cleaves NFR5 at the juxtamembrane domain.

Supplemental Figure 4. Characterization of cleavage site of LysM receptor.

Supplemental Figure 5. The cytoplasmic domains (CDs) of NFR1, NFR5, and kinase–dead NFR1CDK351E were used for kinase assays in E. coli.

Supplemental Figure 6. Mutant version of NFR5 fails to form infections.

Supplemental Figure 7. Phylogenetic tree based on the amino acid sequence of NopT homologs from different bacterial species.

Supplemental Figure 8. Transient expression of NopT triggers cell death in Arabidopsis and Nicotiana tabacum.

Supplemental Table 1. Phosphopeptides identified by Liquid Chromatography–Mass spectrometry.

Supplemental Table 2. Primers used in this study.

Acknowledgments: We greatly thank Prof. Zhongming Zhang for his valuable suggestions in this project. We thank Drs. E. Giraud, E. Wang, and Y. Liang for their critical reading of this manuscript. We thank Dr. J. Staugaard for kindly providing *pNIN:GUS* transgenic seed; Dr. J. Du for providing plasmids expressing of Avr3a and R3a, BAX, and INF1. The qPCR and microscopy data were acquired from the Core Facility Center run by the National Key Lab of Agricultural Microbiology.

Funding: This work was supported by the National Key R&D Program of China (2019YFA0904700), the National Natural Science Foundation of China (32090063), and the Fundamental Research Funds for the Central Universities (2662022SKYJ002). Work in the Stacey's Lab was supported by a grant from National Science Foundation, Plant Genome Research Project (IOS–1734145).

Author Contributions: H.B., Y.C., and G.S. conceived the idea and designed the research, S.F.W. and C.S. provided the NGR234 *nopt* strain; H.B., Y.W., Y.L., and Y.Y.

performed experiments; H.B., Y.W., H. L., H.Z., and Y.C. analyzed the data, Q.W and S.X identified the cleavage site by MS. H.B., Y.C., and G.S. wrote the paper; S.F.W. and C.S. helped to revise the MS.

References

Akeda, Y., and Galán, J.E. (2005). Chaperone release and unfolding of substrates in type III secretion. Nature **437,** 911-915.

Ausmees, N., Kobayashi, H., Deakin, W.J., Marie, C., Krishnan, H.B., Broughton, W.J., and Perret, X. (2004). Characterization of NopP, a type III secreted effector of sp. strain NGR234. J Bacteriol **186,** 4774-4780.

Bos, J.I., Kanneganti, T.D., Young, C., Cakir, C., Huitema, E., Win, J., Armstrong, M.R., Birch, P.R., and Kamoun, S. (2006). The C-terminal half of *Phytophthora infestans* RXLR effector AVR3a is sufficient to trigger R3a-mediated hypersensitivity and suppress INF1-induced cell death in *Nicotiana benthamiana*. Plant J **48,** 165-176.

Bozsoki, Z., Cheng, J., Feng, F., Gysel, K., Vinther, M., Andersen, K.R., Oldroyd, G., Blaise, M., Radutoiu, S., and Stougaard, J. (2017). Receptor-mediated chitin perception in legume roots is functionally separable from Nod factor perception. Proc Natl Acad Sci U S A **114,** E8118-E8127.

Broghammer, A., Krusell, L., Blaise, M., Sauer, J., Sullivan, J.T., Maolanon, N., Vinther, M., Lorentzen, A., Madsen, E.B., Jensen, K.J., Roepstorff, P., Thirup, S., Ronson, C.W., Thygesen, M.B., and Stougaard, J. (2012). Legume receptors perceive the rhizobial lipochitin oligosaccharide signal molecules by direct binding. Proc Natl Acad Sci U S A **109,** 13859-13864.

Cao, Y., Liang, Y., Tanaka, K., Nguyen, C.T., Jedrzejczak, R.P., Joachimiak, A., and Stacey, G. (2014). The kinase LYK5 is a major chitin receptor in *Arabidopsis* and forms a chitin-induced complex with related kinase CERK1. eLife **3**.e03766.

Dai, W.J., Zeng, Y., Xie, Z.P., and Staehelin, C. (2008). Symbiosis-promoting and deleterious effects of NopT, a novel type 3 effector of *Rhizobium* sp. strain NGR234. J Bacteriol **190,** 5101-5110.

Dowen, R.H., Engel, J.L., Shao, F., Ecker, J.R., and Dixon, J.E. (2009). A family of bacterial cysteine protease type III effectors utilizes acylation-dependent and -independent strategies to localize to plasma membranes. J Biol Chem **284,** 15867-15879.

Fotiadis, C.T., Dimou, M., Georgakopoulos, D.G., Katinakis, P., and Tampakaki, A.P. (2012). Functional characterization of NopT1 and NopT2, two type III effectors of *Bradyrhizobium japonicum*. FEMS Microbiol Lett **327,** 66-77.

Gan, Y., Zhang, L., Zhang, Z., Dong, S., Li, J., Wang, Y., and Zheng, X. (2009). The LCB2 subunit of the sphingolip biosynthesis enzyme serine palmitoyltransferase can function as an attenuator of the hypersensitive response and Bax-induced cell death. New Phytol **181,** 127-146.

Geurts, R., Fedorova, E., and Bisseling, T. (2005). Nod factor signaling genes and their function in the early stages of infection. Curr Opin Plant Biol **8,** 346-352.

Goehre, V., Spallek, T., Haeweker, H., Mersmann, S., Mentzel, T., Boller, T., de Torres, M., Mansfield, J.W., and Robatzek, S. (2008). Plant pattern-recognition receptor FLS2 is directed for degradation by the bacterial ubiquitin ligase AvrPtoB. Curr Biol **18,** 1824-1832.

Gysel, K., Laursen, M., Thygesen, M.B., Lironi, D., Bozsoki, Z., Hjuler, C.T., Maolanon, N.N., Cheng, J., Bjork, P.K., Vinther, M., Madsen, L.H., Rubsam, H., Muszynski, A., Ghodrati, A., Azadi, P., Sullivan, J.T., Ronson, C.W., Jensen, K.J., Blaise, M., Radutoiu, S., Stougaard, J., and Andersen, K.R. (2021). Kinetic proofreading of lipochitooligosaccharides determines signal activation of symbiotic plant receptors. Proc Natl Acad Sci U S A **118**.e2111031118.

Han, Y., Sun, J., Yang, J., Tan, Z., Luo, J., and Lu, D. (2017). Reconstitution of the plant ubiquitination cascade in bacteria using a synthetic biology approach. Plant J **91,** 766-776.

Heckmann, A.B., Sandal, N., Bek, A.S., Madsen, L.H., Jurkiewicz, A., Nielsen, M.W., Tirichine, L., and Stougaard, J. (2011). Cytokinin induction of root nodule primordia in *Lotus japonicus* is regulated by a mechanism operating in the root cortex. Mol Plant Microbe Interact **24,** 1385-1395.

Jones, J.D.G., and Dangl, J.L. (2006). The plant immune system. Nature **444,** 323-329.

Kawaharada, Y., Kelly, S., Nielsen, M.W., Hjuler, C.T., Gysel, K., Muszynski, A., Carlson, R.W., Thygesen, M.B., Sandal, N., Asmussen, M.H., Vinther, M., Andersen, S.U., Krusell, L., Thirup, S., Jensen, K.J., Ronson, C.W., Blaise, M., Radutoiu, S., and Stougaard, J. (2015). Receptor-mediated exopolysaccharide perception controls bacterial infection. Nature **523,** 308-312.

Khan, A., Wadood, S.F., Chen, M., Wang, Y., Xie, Z.P., and Staehelin, C. (2022). Effector-triggered inhibition of nodulation: A rhizobial effector protease targets soybean kinase GmPBS1-1. Plant Physiol **189,** 2382-2395.

Kim, S.H., Qi, D., Ashfield, T., Helm, M., and Innes, R.W. (2016). Using decoys to expand the recognition specificity of a plant disease resistance protein. Science **351,** 684-687.

Kimbrel, J.A., Thomas, W.J., Jiang, Y., Creason, A.L., Thireault, C.A., Sachs, J.L., and Chang, J.H. (2013). Mutualistic co-evolution of type III effector genes in Sinorhizobium fredii and *Bradyrhizobium japonicum*. PLoS Pathog **9,** e1003204.

Kopan, R., and Ilagan, M.X.G. (2009). The canonical notch signaling pathway: Unfolding the activation mechanism. Cell **137,** 216-233.

Lei, L., Stevens, D.M., and Coaker, G. (2020). Phosphorylation of the *Pseudomonas* effector AvrPtoB by *Arabidopsis* SnRK2.8 is required for bacterial virulence. Mol Plant **13,** 1513-1522.

Li, D.D., Zhu, Z.K., Deng, X.M., Zou, J.N., Ma, C., Li, C.D., Yin, T., Liu, C.Y., Wang, J.H., Chen, Q.S., and Xin, D.W. (2023). GmPBS1, a hub gene interacting with Rhizobial type-III effectors NopT and NopP, regulates soybean nodulation. Agronomy **13**.1242.

Li, H., Chen, M., Duan, L., Zhang, T., Cao, Y., and Zhang, Z. (2018). Domain swap approach reveals the Ccritical roles of different domains of SYMRK in root nodule symbiosis in *Lotus japonicus*. Front Plant Sci **9,** 697.

Li, L., Kim, P., Yu, L., Cai, G., Chen, S., Alfano, J.R., and Zhou, J.M. (2016). Activation-dependent destruction of a co-receptor by a *Pseudomonas syringae* effector dampens plant immunity. Cell Host Microbe **20,** 504-514.

Madsen, E.B., Madsen, L.H., Radutoiu, S., Olbryt, M., Rakwalska, M., Szczyglowski, K., Sato, S., Kaneko, T., Tabata, S., Sandal, N., and Stougaard, J. (2003). A receptor kinase gene of the LysM type is involved in legume perception of rhizobial signals. Nature **425,** 637-640.

Madsen, E.B., Antolin-Llovera, M., Grossmann, C., Ye, J., Vieweg, S., Broghammer, A., Krusell, L., Radutoiu, S., Jensen, O.N., Stougaard, J., and Parniske, M. (2011). Autophosphorylation is essential for the *in vivo* function of the *Lotus japonicus* Nod factor receptor 1 and receptor-mediated signalling in cooperation with Nod factor receptor 5. Plant J **65,** 404-417.

Moling, S., Pietraszewska-Bogiel, A., Postma, M., Fedorova, E., Hink, M.A., Limpens, E., Gadella, T.W., and Bisseling, T. (2014). Nod factor receptors form heteromeric complexes and are essential for intracellular infection in medicago nodules. Plant Cell **26,** 4188-4199.

Nakagawa, T., Suzuki, T., Murata, S., Nakamura, S., Hino, T., Maeo, K., Tabata, R., Kawai, T., Tanaka, K., Niwa, Y., Watanabe, Y., Nakamura, K., Kimura, T., and Ishiguro, S. (2007). Improved Gateway binary vectors: high-performance vectors for creation of fusion constructs in transgenic analysis of plants. Biosci Biotechnol Biochem **71,** 2095-2100.

Ntoukakis, V., Mucyn, T.S., Gimenez-Ibanez, S., Chapman, H.C., Gutierrez, J.R., Balmuth, A.L., Jones, A.M., and Rathjen, J.P. (2009). Host inhibition of a bacterial virulence effector triggers immunity to infection. Science **324,** 784-787.

Schmidt, G. (2011). Yersinia enterocolitica outer protein T (YopT). Eur J Cell Biol **90,** 955-958.

Schubert, K.A., Xu, Y., Shao, F., and Auerbuch, V. (2020). The type III secretion system as a tool for studying cytosolic innate immune surveillance. Ann Rev Microbiol, Vol 74, 2020 **74,** 221-245.

Shao, F., Merritt, P.M., Bao, Z., Innes, R.W., and Dixon, J.E. (2002). A *Yersinia* effector and a *Pseudomonas* avirulence protein define a family of cysteine proteases functioning in bacterial pathogenesis. Cell **109,** 575-588.

Shao, F., Vacratsis, P.O., Bao, Z., Bowers, K.E., Fierke, C.A., and Dixon, J.E. (2003a). Biochemical characterization of the *Yersinia* YopT protease: cleavage site and recognition elements in Rho GTPases. Proc Natl Acad Sci U S A **100,** 904-909.

Shao, F., Golstein, C., Ade, J., Stoutemyer, M., Dixon, J.E., and Innes, R.W. (2003b). Cleavage of *Arabidopsis* PBS1 by a bacterial type III effector. Science **301,** 1230-1233.

Sugawara, M., Takahashi, S., Umehara, Y., Iwano, H., Tsurumaru, H., Odake, H., Suzuki, Y., Kondo, H., Konno, Y., Yamakawa, T., Sato, S., Mitsui, H., and Minamisawa, K. (2018). Variation in bradyrhizobial NopP effector determines symbiotic incompatibility with soybeans via effector-triggered immunity. Nature Commun **9**.3139.

Sun, Y., Li, L., Macho, A.P., Han, Z., Hu, Z., Zipfel, C., Zhou, J.-M., and Chai, J. (2013). Structural basis for flg22-induced activation of the *Arabidopsis* FLS2-BAK1 immune complex. Science **342,** 624-628.

Tang, D.Z., Wang, G.X., and Zhou, J.M. (2017). Receptor kinases in plant-pathogen interactions: More than pattern recognition. Plant Cell **29,** 618-637.

Teulet, A., Busset, N., Fardoux, J., Gully, D., Chaintreuil, C., Cartieaux, F., Jauneau, A., Comorge, V., Okazaki, S., Kaneko, T., Gressent, F., Nouwen, N., Arrighi, J.F.,

Koebnik, R., Mergaert, P., Deslandes, L., and Giraud, E. (2019). The rhizobial type III effector ErnA confers the ability to form nodules in legumes. Proc Natl Acad Sci U S A **116,** 21758-21768.

Vleeshouwers, V.G., Driesprong, J.D., Kamphuis, L.G., Torto-Alalibo, T., Van't Slot, K.A., Govers, F., Visser, R.G., Jacobsen, E., and Kamoun, S. (2006). Agroinfection-based high-throughput screening reveals specific recognition of INF elicitins in *Solanum*. Mol Plant Pathol **7,** 499-510.

Wang, D., Yang, S., Tang, F., and Zhu, H. (2012). Symbiosis specificity in the legume: rhizobial mutualism. Cell Microbiol **14,** 334-342.

Wang, Q., Han, C., Ferreira, A.O., Yu, X., Ye, W., Tripathy, S., Kale, S.D., Gu, B., Sheng, Y., Sui, Y., Wang, X., Zhang, Z., Cheng, B., Dong, S., Shan, W., Zheng, X., Dou, D., Tyler, B.M., and Wang, Y. (2011). Transcriptional programming and functional interactions within the *Phytophthora sojae* RXLR effector repertoire. Plant Cell **23,** 2064-2086.

Xiang, T., Zong, N., Zou, Y., Wu, Y., Zhang, J., Xing, W., Li, Y., Tang, X., Zhu, L., Chai, J., and Zhou, J.M. (2008). *Pseudomonas syringae* effector AvrPto blocks innate immunity by targeting receptor kinases. Curr Biol **18,** 74-80.

Xu, N., Luo, X., Wu, W., Xing, Y., Liang, Y., Liu, Y., Zou, H., Wei, H.L., and Liu, J. (2020). A plant lectin receptor-like kinase phosphorylates the bacterial effector AvrPtoB to dampen Iits virulence in *Arabidopsis*. Mol Plant **13,** 1499-1512.

Yang, J., Lan, L., Jin, Y., Yu, N., Wang, D., and Wang, E. (2022). Mechanisms underlying legume-rhizobium symbioses. J Integr Plant Biol **64,** 244-267.

Zhang, B., Wang, M., Sun, Y., Zhao, P., Liu, C., Qing, K., Hu, X., Zhong, Z., Cheng, J., Wang, H., Peng, Y., Shi, J., Zhuang, L., Du, S., He, M., Wu, H., Liu, M., Chen, S., Wang, H., Chen, X., Fan, W., Tian, K., Wang, Y., Chen, Q., Wang, S., Dong, F., Yang, C., Zhang, M., Song, Q., Li, Y., and Wang, X. (2021). *Glycine max* NNL1 restricts

symbiotic compatibility with widely distributed *Bradyrhizobia via* root hair infection. Nat Plants **7,** 73-86.

Zhang, J., Li, W., Xiang, T., Liu, Z., Laluk, K., Ding, X., Zou, Y., Gao, M., Zhang, X., Chen, S., Mengiste, T., Zhang, Y., and Zhou, J.M. (2010). Receptor-like cytoplasmic kinases integrate signaling from multiple plant immune receptors and are targeted by a *Pseudomonas syringae* effector. Cell Host Microbe **7,** 290-301.

Zhou, J.G., Wang, P., Claus, L.A.N., Savatin, D.V., Xu, G.Y., Wu, S.J., Meng, X.Z., Russinova, E., He, P., and Shan, L.B. (2019). Proteolytic orocessing of SERK3/BAK1 regulates plant immunity, development, and cell death. Plant Physiol **180,** 543-558.

Zipfel, C., and Oldroyd, G.E.D. (2017). Plant signalling in symbiosis and immunity. Nature **543,** 328-336.

Zipfel, C., Robatzek, S., Navarro, L., Oakeley, E.J., Jones, J.D.G., Felix, G., and Boller, T. (2004). Bacterial disease resistance in through flagellin perception. Nature **428,** 764-767.

Supplemental Figures

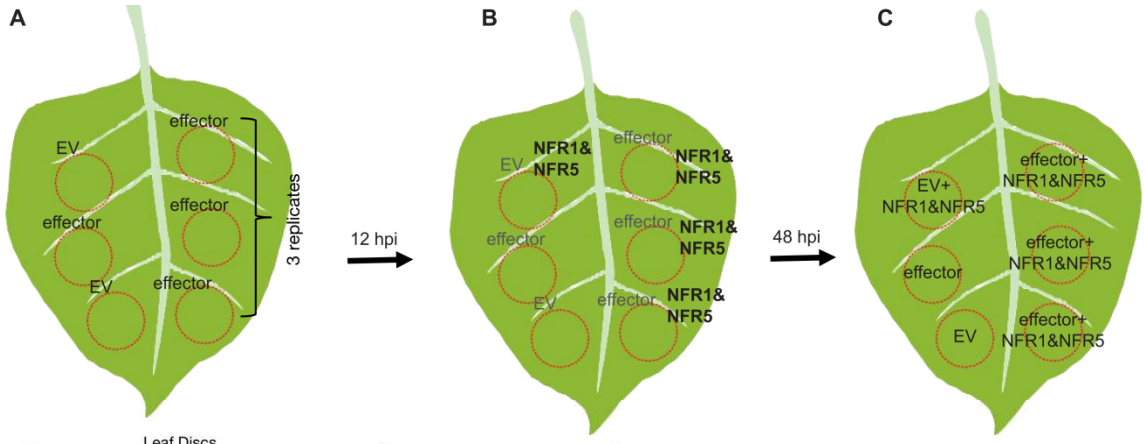

D

Effector	Leaf Discs (Cell death/total) Ctrl.	NFR1&NFR5
NopA	0/3	9/9
NopB	0/3	9/9
NopC	0/3	9/9
NopJ	0/3	9/9
NopL	0/3	9/9
NopM	3/3	9/9
NopP	0/3	9/9
NopT	0/3	0/9
NopU	0/3	9/9
NopV	0/3	9/9
NopX	0/3	9/9
NopY	0/3	9/9
NopZ	0/3	4/9
NopBE	0/3	9/9
NopBI	0/3	9/9

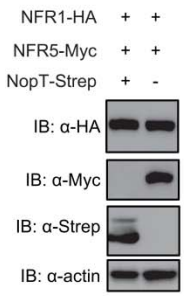

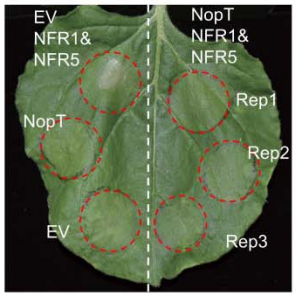

Supplemental Fig. 1. Analyses of the functions of all 15 effectors from *S. fredii* NGR234 in preventing LjNFR1- and LjNFR5-induced cell death in *N. benthamiana* leaves.

15 genes from *S. fredii* NGR234 encoding effector proteins were amplified and cloned into binary vector for expression of Strep-tagged proteins in *N. benthamiana*. LjNFR1 and LjNFR5 from *L. japonicus* were C-terminally tagged with HA and Myc, respectively, and cloned into binary vectors for expression in *N. benthamiana*. All plasmids were electroporated into *Agrobacterium tumefaciens* EH105.

(A) *Agrobacterium* strain harboring each effector gene or control empty vector (EV) were infiltrated into *N. benthamiana*. 12 hour post infiltration (hpi), agrobacterium strains harboring LjNFR1 and LjNFR5 were mixed and hand-infiltrated in the same leaf discs as shown in (B). 48 hpi, cell death

phenotypes were evaluated (C). At least three replicates in the same leaf were performed to test the function of each effector in suppressing cell death-triggered by LjNFR1 and LjNFR5. (D) Results of all 15 effector proteins in suppressing programmed cell death by overexpression of NFR1 and NFR5. (E) Abundance of LjNFR1, LjNFR5, and NopT proteins, as measured by immunoblot with specific antibodies. Leaf discs expressing LjNFR1, LjNFR5, and NopT or LjNFR1 and LjNFR5 and with EV were used for immunoblot analyses. Actin was used as loading control. (F) Another example of suppression of programmed cell death by NopT in the leaf discs coexpressing NFR1 and NFR5. Rep1, Rep2, and Rep3 represent three technical repeats in the same leave.

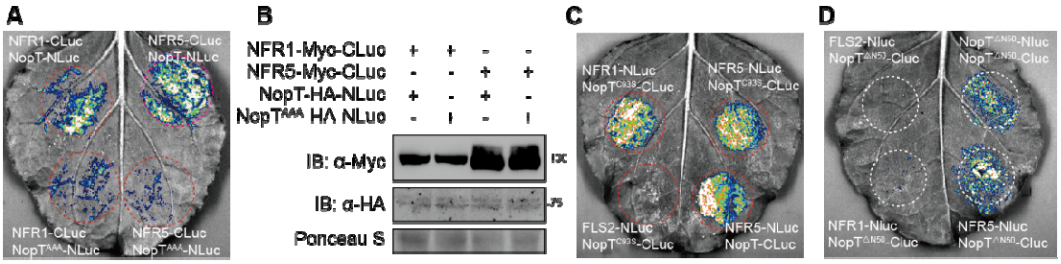

Supplemental Fig. 2. Split–LUC assay testing the interactions between different NopT mutants and NFRs.

(A)The interaction between NopT with mutated acylation site and NFR1/NFR5. $NopT^{AAA}$ (G50A C51A C52A). (B) The protein expressing of indicating genes in the leave of (A). (C) Nop^{C93S} interact with NFR1 and NFR5. (D) The interaction between $NopT^{\Delta N50}$ and NFR5. $NopT^{\Delta N50}$ represents a truncated NopT with deletion of about 50 a.a. from its N–terminus.

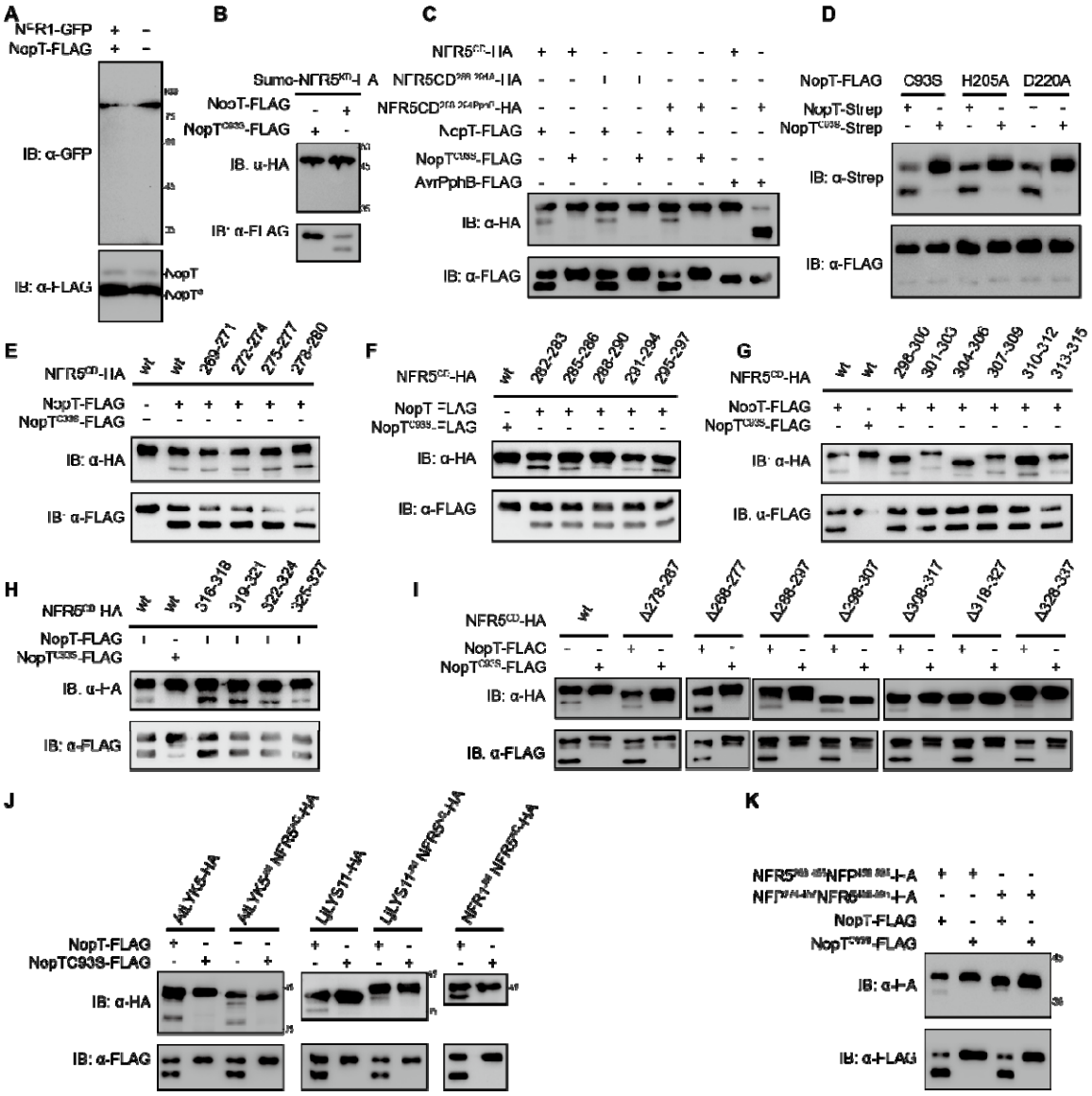

Supplemental Fig. 3. NopT cleaves NFR5 at the juxtamembrane domain.

(A) NopT cannot cleave NFR1-GFP expressed in *N. benthamiana* leaves. recombinant Sumo-NFR5^{KD}-HA lacking the juxtamembrane (JM) domain. (B) NopT could not cleave Sumo–NFR5^{KD}–HA, a recombinant protein expressed in *E. coli* with the juxtamembrane domain of NFR5 was replaced with Sumo tag. (C) Cleavage assay using two mutant versions of NFR5^{CD} in the presence of NopT or AvrPphB. NFR5$^{CD288-294A}$ represents a mutant NFR5^{CD} with residues 288 to 294 replaced with seven alanines; NFR5$^{CD288-294PphB}$ represents a mutant NFR5^{CD} with residues 288 to 294 replaced with AvrPphB recognition

sites. (D) Autocleavage assay, using different NopT variants with single amino acid mutations. H205A and D220A indicate His-205 and Asp-220 replaced with alanine, respectively. (E-H) NopT cleavage assay using 19 variants of $NFR5^{CD}$ with three adjacent amino acids replaced with three alanines. The numbers indicate the location of the three residues replaced with alanines. (I) NopT cleavage assay using seven truncated variants of $NFR5^{CD}$ with 10 adjacent amino acids deleted. The numbers indicate the location of the 10 deleted residues. (J) NopT but not $NopT^{C93S}$ could cleave the CDs of AtLYK5 and LjLYS11 expressed in E. coli. NopT could cleave both $AtLYK5^{JM}$–$NFR5^{KC}$, $LjLYS11^{JM}$–$NFR5^{KC}$ and $LjNFR1^{JM}$–$NFR5^{KC}$, three recombinant proteins expressed in *E. coli* with the JM of NFR5 was replaced with the JMs from AtLYK5, LjLYS11 and NFR1, respectively. (K) NopT but not $NopT^{C93S}$ could cleave recombinant protein $NFR5^{268\text{-}445}$-$NFP^{458\text{-}595}$ and $NFP^{270\text{-}457}$-$NFR^{5456\text{-}595}$.

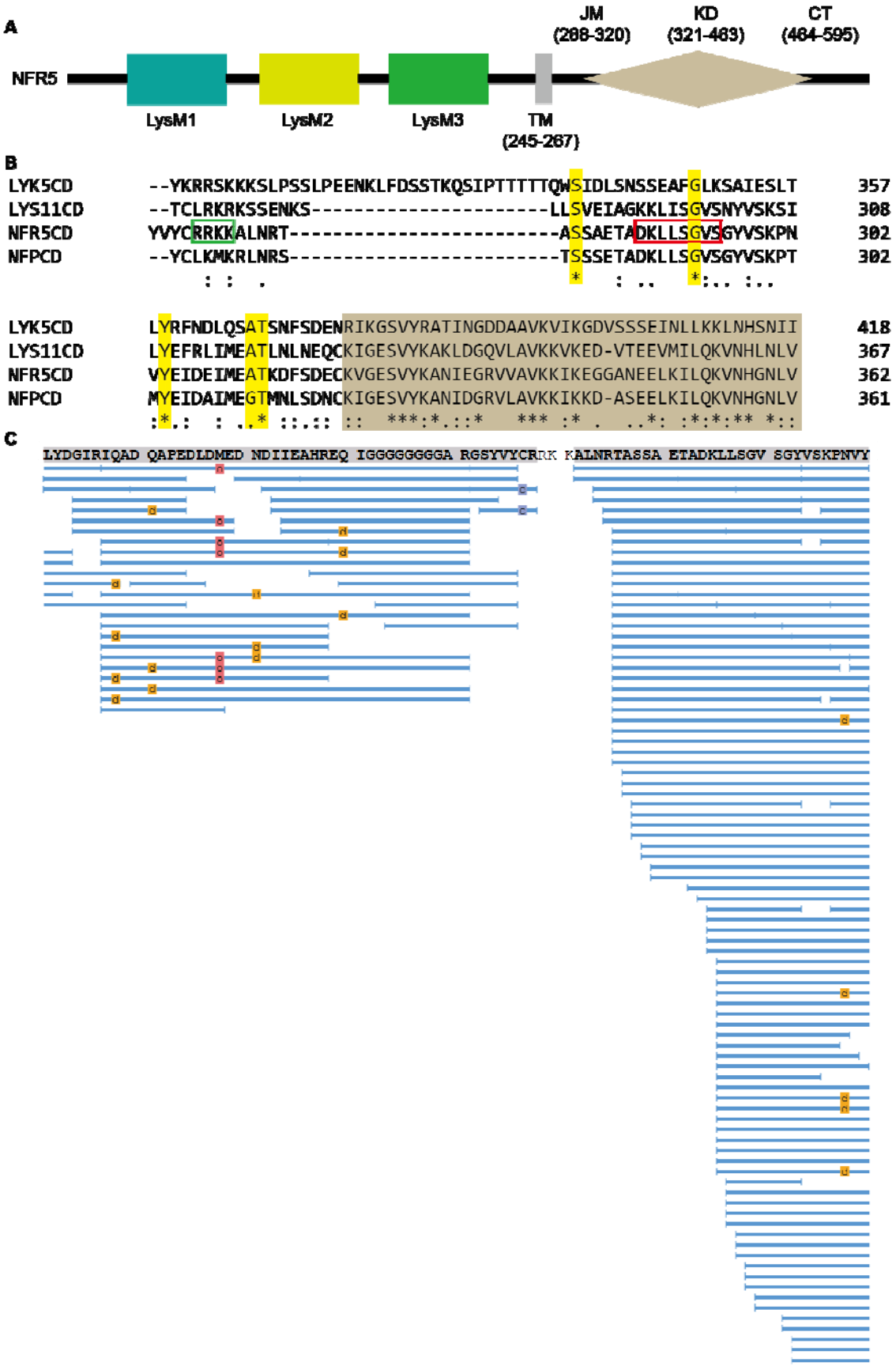
A
JM
(288-320)
KD
(321-483)
CT
(484-595)
NFR5
LysM1
LysM2
LysM3
TM
(245-267)
B
LYK5CD --YKRRSKKKSLPSSLPEENKLFDSSTKQSIPTTTTTQWSIDLSNSSEAFGLKSAIESLT 357
LYS11CD --TCLRKRKSSENKS----------LLSVEIAGKKLISGVSNYVSKSI 308
NFR5CD YVYCRRKKALNRT----------ASSAETADKLLSGVSGYVSKPN 302
NFPCD --YCLKMKRLNRS----------TSSSETADKLLSGVSGYVSKPT 302
LYK5CD LYRFNDLQSATSNFSDENRIKGSVYRATINGDDAAVKVIKGDVSSSEINLLKKLNHSNII 418
LYS11CD LYEFRLIMEATLNLNEQCKIGESVYKAKLDGQVLAVKKVKED-VTEEVMILQKVNHLNLV 367
NFR5CD VYEIDEIMEATKDFSDECKVGESVYKANIEGRVVAVKKIKEGGANEELKILQKVNHGNLV 362
NFPCD MYEIDAIMEGTMNLSDNCKIGESVYKANIDGRVLAVKKIKKD-ASEELKILQKVNHGNLV 361
C
LYDGIRIQAD QAPEDLDMED NDIIEAHREQ IGGGGGGGGA RGSYVYCRRK KALNRTASSA ETADKLLSGV SGYVSKPNVY

Supplemental Fig. 4. Characterization of cleavage site of LysM receptor.

(A) Domain and motif annotation of NFR5. (B) Protein sequence alignment of the cytoplasmic domain of AtLYK5, LjLYS11, LjNFR5 and MtNFP. Yellow boxes delineated highly conserved residues (S283, G294, Y303, A310, T311) and brown box delineated kinase domain. Green frame delineated cleavage site of NFR5 and red frame delineated residues similar to NopT autocleavage region. (C) Mass spectrometry analysis of cleaved NFR5. Blue lines indicated the peptides characterized by MS.

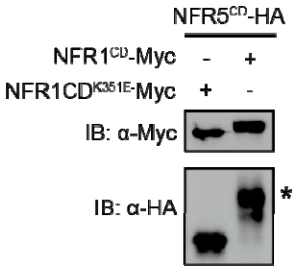

Supplemental Fig. 5. The cytoplasmic domains (CDs) of NFR1, NFR5, and kinase–dead NFR1CD^{K351E} were used for kinase assays in *E. coli*. Proteins were detected by immunoblotting using anti–HA and anti–Myc antibodies. Asterisk indicated the band retardation on the gel representing the phosphorylated NFR5^{CD} proteins.

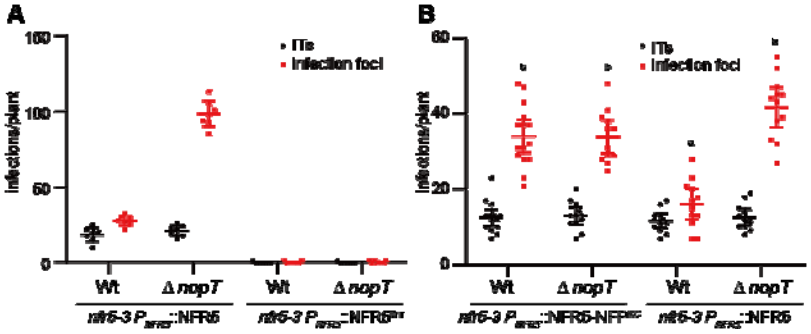

Supplemental Fig. 6. Rhizobial infection in the mutant versions of NFR5.

(A) NFR5^{5m} failed to form rhizobial infection (n=7, Student's *t*–test: $P < 0.01$). (B)NFR5-NFP^{KD-CT} could recuse the rhizobial infection of wild type NGR234 (n=10, Student's t–test: $P < 0.01$). The transgenic roots expressing NFR5 or NFR5^{5m} or NFR5-NFP^{KCT} in the *nfr5-3* mutant under the control of native promoter were inoculated with GFP-labelled wild type NGR234 and NGR234Δ*nopT* respectively. The data was collected 9 days post inoculation.

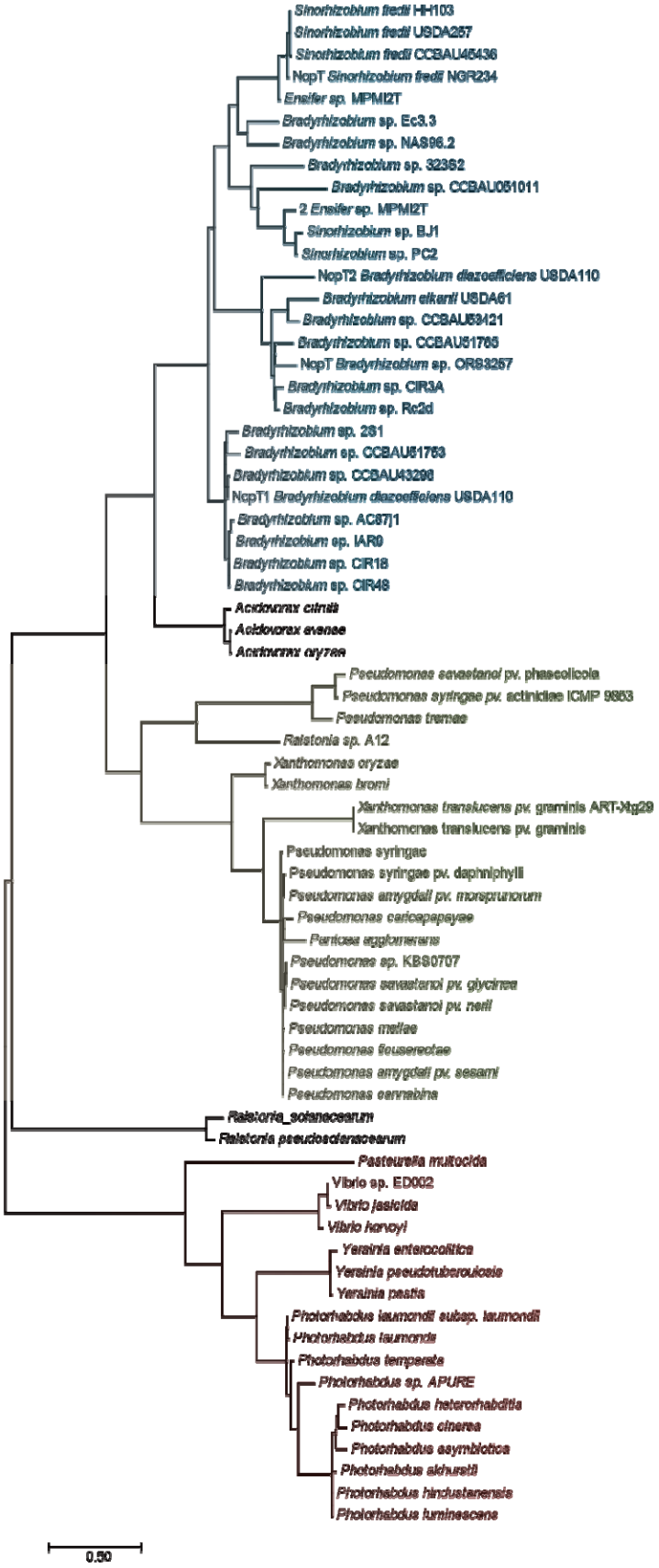
Sinorhizobium fredii HH103
Sinorhizobium fredii USDA257
Sinorhizobium fredii CCBAU45436
NopT Sinorhizobium fredii NGR234
Ensifer sp. MPMI2T
Bradyrhizobium sp. Ec3.3
Bradyrhizobium sp. NAS96.2
Bradyrhizobium sp. 32362
Bradyrhizobium sp. CCBAU051011
2 Ensifer sp. MPMI2T
Sinorhizobium sp. BJ1
Sinorhizobium sp. PC2
NopT2 Bradyrhizobium diazoefficiens USDA110
Bradyrhizobium elkanii USDA61
Bradyrhizobium sp. CCBAU53421
Bradyrhizobium sp. CCBAU51765
NopT Bradyrhizobium sp. ORS3257
Bradyrhizobium sp. CIR3A
Bradyrhizobium sp. Rc2d
Bradyrhizobium sp. 2S1
Bradyrhizobium sp. CCBAU51753
Bradyrhizobium sp. CCBAU43298
NopT1 Bradyrhizobium diazoefficiens USDA110
Bradyrhizobium sp. AC87j1
Bradyrhizobium sp. IAR9
Bradyrhizobium sp. CIR18
Bradyrhizobium sp. CIR48
Acidovorax citrulli
Acidovorax avenae
Acidovorax oryzae
Pseudomonas savastanoi pv. phaseolicola
Pseudomonas syringae pv. actinidiae ICMP 9853
Pseudomonas tremae
Ralstonia sp. A12
Xanthomonas oryzae
Xanthomonas bromi
Xanthomonas translucens pv. graminis ART-Xtg29
Xanthomonas translucens pv. graminis
Pseudomonas syringae
Pseudomonas syringae pv. daphniphylli
Pseudomonas amygdali pv. morsprunorum
Pseudomonas caricapapayae
Pantoea agglomerans
Pseudomonas sp. KBS0707
Pseudomonas savastanoi pv. glycinea
Pseudomonas savastanoi pv. nerii
Pseudomonas mellae
Pseudomonas fluorescens
Pseudomonas amygdali pv. sesami
Pseudomonas cannabina
Ralstonia_solanacearum
Ralstonia pseudosolanacearum
Pasteurella multocida
Vibrio sp. ED002
Vibrio jasicida
Vibrio harveyi
Yersinia enterocolitica
Yersinia pseudotuberculosis
Yersinia pestis
Photorhabdus laumondii subsp. laumondii
Photorhabdus laumondii
Photorhabdus temperata
Photorhabdus sp. APURE
Photorhabdus heterorhabditis
Photorhabdus cinerea
Photorhabdus asymbiotica
Photorhabdus akhurstii
Photorhabdus hindustanensis
Photorhabdus luminescens
0.50

1060

Supplemental Fig. 7. Phylogenetic tree based on the amino acid sequence of NopT homologs from different bacterial species.

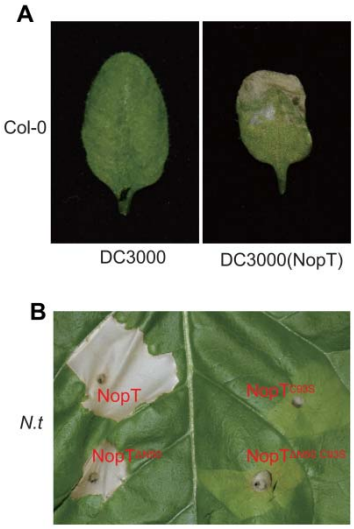

Supplemental Fig. 8. Transient expression of NopT triggers cell death in *Arabidopsis thaliana* and *Nicotiana tabacum*.

(A) *Pseudomonas syringae* pv tomato DC3000 harboring control plasmids (left) or expressing NopT (right) were infiltrated into Arabidopsis leaves. Note the cell death in the right-side panel. (B) *Agrobacterium* strains harboring *NopT*, *NopT* with an N-terminal 50–amino acid deletion, $NopT^{C93S}$, or $NopT^{C93S}$ with an N-terminal 50–amino acid deletion were infiltrated into *N. tabacum* leaves.

Supplemental Table 1. Phosphopeptides identified by liquid chromatography–mass spectrometry. An *in vitro* kinase assay was performed using the CD of NFR1 and NopT. NopT was separated by SDS-PAGE, and the digested gel slices representing the phosphorylated NopT were used for analysis. The deduced phosphopeptides are listed.

Sequence	Modifications	SITE	PSMs_NFR1KE+NopT	PSMs_NFR1+NopT
ETLANVELRTK	1xPhospho [T10]	37T	-	1
ETLANVELR	1xPhospho [T2]	29T	-	1
ETLANVELRTKSPSAECPDK	1xCarbamidomethyl [C17]; 1xPhospho [T10]	37T	-	1
TKSPSAECPDK	1xCarbamidomethyl [C8]; 1xPhospho [S5]	41S	-	1
SPSAECPDK	1xCarbamidomethyl [C6]; 1xPhospho [S3]	41S		1
SPSAECPDKMGCCASKPQASDPNNPSTSSPARPSTSLFR	3xCarbamidomethyl [C6; C12; C13]; 1xOxidation [M10]		1	1
SPSAECPDKMGCCASKPQASDPNNPSTSSPARPSTSLFR	3xCarbamidomethyl [C6; C12; C13]; 1xPhospho [S/T]; 1xOxidation [M10]		-	4
MGCCASKPQASDPNNPSTSSPARPSTSLFR	2xCarbamidomethyl [C3; C4]; 1xPhospho [T/S]; 1xOxidation [M1]		-	11
MGCCASKPQASDPNNPSTSSPARPSTSLFR	2xCarbamidomethyl [C3; C4]; 1xPhospho [T/S]		-	9
MGCCASKPQASDPNNPSTSSPARPSTSLFR	2xCarbamidomethyl [C3; C4]; 2xPhospho [T/S]	65S 66T	-	4
MGCCASKPQASDPNNPSTSSPARPSTSLFR	2xCarbamidomethyl [C3; C4]; 1xOxidation [M1]		4	2
MGCCASKPQASDPNNPSTSSPARPSTSLFR	2xCarbamidomethyl [C3; C4]; 2xPhospho [T/S]; 1xOxidation [M1]		-	4
TAELAQANADGICVGLTAEWLR	1xCarbamidomethyl [C13]; 1xPhospho [T17]	97T	-	10
NLNSHPSIR	1xPhospho [S7]	109S	-	2
NLNSHPSIRMEALVPGSQR	1xPhospho [S7]; 1xOxidation [M10]	119S	-	1
MEALVPGSQR	1xPhospho [S8]	119S	-	1
MEALVPGSQR	1xPhospho [S8]; 1xOxidation [M1]	119S	-	1
RQGAGPSEADFAAQNTMLQK	1xPhospho [T/S]; 1xOxidation [M17]		-	3
RQGAGPSEADFAAQNTMLQK	1xPhospho [T16]	156T	-	2
QGAGPSEADFAAQNTMLQK	1xPhospho [T/S]; 1xOxidation [M16]		-	3
QGAGPSEADFAAQNTMLQK	1xPhospho [T15]	156T	-	2
SLANRYSNPNR	1xPhospho [S7]	245S	-	2
QHLTTVTTQK	1xPhospho [T8]	257T	-	1

Supplemental Table 2. Primers used in this study.

Used for	Target genes	Names	Sequences (from 5' to 3')
Overexpression in Nicotiana benthamiana	NopT or NopT^{C93S}	p5X-NopT-F	agaacacgggggactctagaatgcacagtcccatcag
		p5X-NopT-R	ccgctgttatcggtacctgtcatcttttgggtggtcac
	NopT$^{\Delta N50}$	p5X-NopTN50-F	agaacacgggggactctagaatgtgctgcgccagcaag
	NFR1	p5X-NFR1-F	agaacacgggggactctagaatgaagctaaaaactggtctact
		p5X-NFR1-R	ccgctgttatcggtacctcttctcacagac
	NFR5	p5X-NFR5-F	agaacacgggggactctagaatggctgtcttctttcttacc
		p5X-NFR5-R	ccgctgttatcggtaccacgtgcagtaat
		p5X-NFR5gfp-R	tcccgggagcggtaccacgtgcagtaatggaagt
	AvrPphB	p5X-AvrPphB-F	agaacacgggggactctagaatgaaaataggtacgcaggcc
		p5X-AvrPphB-R	ccgctgttatcggtacccgaaactctaaactcgtttacgc
templates for protein expression	NopT$_{USDA257}$	p5X-257T-F	agaacacgggggactctagatgctgcgtgatccgaacaat
		p5X-257T-R	ccgctgttatcggtacctgtcacctttgggtggtcaccg
	NopT1$_{USDA110}$	p5X-110T1-F	agaacacgggggactctagaatgtatgatcgaatcggtgg
		p5X-110T1-R	ccgctgttatcggtaccctgcatcctttgcgtcg
	NopT2$_{USDA110}$	p5X-110T2-F	agaacacgggggactctagaatgtataatcgagtcgatggc
		p5X-110T2-R	ccgctgttatcggtaccccgatgaggttccgc
Protein Expression in *E.coli*	NopT or NopT^{C93S}	28a NopT-F	tgggtcgcggatccgaattcatgcacagtcccatcag
		28a FLAG-R	tcgagtgcggccgcaagcttcttgtcatcgtcatccttgtag
		28a Strep-R	tcgagtgcggccgcaagctttttttcaaattgaggatgagaccatcc
	AvrPphB	ET28a-pphb-F	tgggtcgcggatccgaattcaaaataggtacgcaggccac
	NopT$_{USDA257}$	ET28a-257T-F	tgggtcgcggatccgaattcctgcgtgatccgaacaa
	NopT1$_{USDA110}$	ET28a-110T1-F	tgggtcgcggatccgaattctatgatcgaatcggtggctc
	NopT2$_{USDA110}$	ET28a-110T2-F	tgggtcgcggatccgaattctataatcgagtcgatggcgaatac
	NFR1CD	duet NFR1-F	accacagccaggatccgagataccagaagaaggaagaagagaaagc
		duet Sac1nost-R	ggcgcgccgagctcgcgatcggggaaattcgagct
		MAL-NFR1-F	ggaaggatttcagaattcggatccagataccagaagaaggaagaagag
		MAL-NFR1-R	cgacggccagtgccaagctttcatcttctcacagacagtaaatttatgag
	NFR5CD	ACSH-NFR5-F	agaagcgcggatccgaattctatgtatactgccgcagaaagaag
		ACSH-NFR5-R	cgtatgggtagcttccaagcttacgtgcagtaatggaagtc
		MAL-NFR5-F	ggaaggatttcagaattcggatcctatgtatactgccgcagaaagaag
		MAL-NFR5-R	cgacggccagtgccaagctttcaacgtgcagtaatggaagtc
	NFR5KD	SUMO 5KD-F	ccgcgaacagattggtaaggttggggaatcagtgtac
		SUMO HA-R	gctcgaattcggatcctttcacgcatagtcaggaacatcg
	NFR5JM	SUMO 5JM-F	ccgcgaacagattggttatgtatactgccgcagaaagaag
		SUMO 5JM-R	gctcgaattcggatcctttcacgcatagtcaggaacatcg
	sumo-NFR5KD-HA	duet sumo-F	catcaccacagccaggatgggtccctgcaggac
		duet HA-R	cattatgcggccgcaagcttttacgcatagtcaggaacatcg
	sumo-NFR5JM-GFP	duet sumo-F	catcaccacagccaggatgggtccctgcaggac
		duet GFP-R	atgcggccgcaagcttttacttgtacaactcatccatacc

	AtLYK5	ACSH-LYK5-F	gcgcggatccgaattctacaaacgaaggtctaagaag
		ACSH-LYK5-R	ggtagcttccaagcttgttgccaagagagccg
	LjLYS11	ACSH-LYS11-F	agaagcgcggatccgaattcacttgtctgaggaagagaaag
		ACSH-LYS11-R	cgtatgggtagcttccaagcttacgagctgctatcaaagtt
	LYK5JM NFR5KD	LYK5-NFR5-F	cgaaaacagaaaggttggggaatcagtg
		NFR5 LYK5-R	ccccaacctttctgttttcgtcgctgaaatt
	LYS11JM NFR5KD	LYS11 NFR5-F	gagcagtgtaaggttggggaatcag
		NFR5 LYS11R	ccccaaccttacactgctcattgagg
site mutantions construction	NopT	T93S-F	gaatctccgtcggcttgactgc
		T93S-F	gacggagattccatctgcgttc
		97D-F	ggcttggatgcggagtggctgcg
		97D-R	ctccgcatccaagccgacgcag
		97A-F	ggcttggctgcggagtggctgc
		97A-R	ctccgcagccaagccgacg
		109D-F	catccggatatccgaatggaggccctag
		109D-R	ttcggatatccggatgactgttgaggttacgc
		109A-F	catccggcaatccgaatggag
		109A-R	ttcggattgccggatgactgttg
		119D-R	cccggagatcaaaggcacgcctcagc
		119A-F	gcctttgatctccgggtactagggcc
		119A-F	cccggagcgcaaaggcac
		119A-R	ctttgcgctccgggtactagg
		156D-F	gcaaaacgatatgttgcagaaagcaggc
		156D-R	gcaacatatcgttttgcgccgcgaagtcggcc
		156A-F	gcaaaacgctatgttgcagaaagcag
		156A-R	ctgcaacatagcgttttgcgccgcgaagtc
		H205A-F	ggcggcaacaccgttgcgacc
		H205A-R	caacggtgttgccgccgccctcagc
		D220A-F	ctcttcgctcctaatttcggcgaatttac
		D220A-R	gccgaaattaggagcgaagagcgtggtgtttc
		245D-F	cgctacgacaatccaaaccggcag
		245D-R	ttggattgtcgtagcgattggctaggct
		257 mutants	changing the sequence of R primer at $nopt_{257}$when cloned into vectors
	NFR1	K351E-F	gcaattgagaagatggatgtacaagcatc
		K351E-R	catccatcttctcaattgctgttttcttgcc
	NFR5	269-271A-F	ctatgcagctgcacgcagaaagaaggctctg
		269-271A-R	gcgtgcagctgcatagaattcggatccgcgc
		272-274A-F	ctgcgctgcagctaaggctctgaataggactgc
		272-274A-R	cttagctgcagcgcagtatacatagaattcggatcc

		275-277A-F	gaaaggcagctgcaaataggactgcttcatcagc
		275-277A-R	ctatttgcagctgcctttctgcggcagtatacatag
		278-280A-F	ctggctgcagctgcttcatcagctgagactg
		278-280A-R	agcagctgcagccagagccttctttctgcg
		282-283A-F	gcagcagctgagactgctgataaactac
		282-283A-R	gcagtctcagctgctgcagcagtcctattcagag
		285-286A-F	ggggctgctgataaactactttctggag
		285-286A-R	agtagtttatcagcagccccagctgatgaagcagtc
		288-290A-F	gctgcagcactttctggagtttcaggctatgtaag
		288-290A-R	aaactccagaaagtgctgcagcagcagtctcagctgatgaag
		291-294A-F	gagactgctgataaactagctgctgcagtttcaggctatgtaagcaagcc
		291-294A-R	atagcctgaaactgcagcagctagtttatcagcagtctcagctg
		295-298A-F	gagttgcagctgctgtaagcaagccaaacgtgtatg
		295-298A-R	cttacagcagctgcaactccagaaagtagtttatcagcag
		298-300A-F	ctatgcagctgcaccaaacgtgtatgaaatcgacg
		298-300A-R	gtttggtgcagctgcatagcctgaaactccagaaagtag
		301-303A-F	gcaaggcagctgcttatgaaatcgacgagataatggaagc
		301-303A-R	cataagcagctgccttgcttacatagcctgaaactcc
		304-306A-F	gtggctgcagctgacgagataatggaagctacgaag
		304-306A-R	cgtcagctgcagccacgtttggcttgcttacatagc
		307-309A-F	gaaatcgctgcagcaatggaagctacgaaggatttcag
		307-309A-R	ccattgctgcagcgatttcatacacgtttggcttgc
		310-312A-F	cgagatagcagctgctacgaaggatttcagcg
		310-312A-R	gtagcagctgctatctcgtcgatttcatacacgtttg
		313-315A-F	gctgcagctgcattcagcgatgagtgcaagg
		313-315A-R	ctgaatgcagctgcagcttccattatctcgtcgatttc
		316-318A-F	ggatgcagctgctgagtgcaaggttggggaatc
		316-318A-R	ctcagcagctgcatccttcgtagcttccattatctc
		319-321A-F	cgatgctgcagctgttggggaatcagtgtacaagg
		319-321A-R	caacagctgcagcatcgctgaaatccttcgtagc
		322-324A-F	gcaaggcagctgcatcagtgtacaaggccaacatag
		322-324A-R	gatgcagctgccttgcactcatcgctgaaatc
		325-327A-F	gaagcagctgcaaaggccaacatagaaggtcg
		325-327A-R	gcctttgcagctgcttccccaaccttgcactc
		268-277DE-F	agaagcgcggatccgaattcaataggactgct
		268-277DE-R	ctgatgaagcagtcctattgaattcggatccgcgcttc
		278-287DE-F	gcagaaagaaggctctggataaactactttctggagtttcagg
		278-287DE-R	aaactccagaaagtagtttatccagagccttctttctgcg
		298-307DE-F	caggctatgagataatggaagctacgaaggatttc
		298-307DE-R	cttccattatctcatagcctgaaactccagaaagtag

			308-317DE-F	gaaatcgacgatgagtgcaaggttgggg
			308-317DE-R	ttgcactcatcgtcgatttcatacacgtttggc
			318-327DE-F	gatttcagcaaggccaacatagaaggtcg
			318-327DE-R	gttggccttgctgaaatccttcgtagcttcc
			328-337DE-F	tcagtgtacgtaaagaaaatcaaggaaggtggtgcc
			328-337DE-R	attttctttacgtacactgattccccaaccttg
			288-294A-F	gcagctgccgcagcggctgcctcaggctatgtaagcaagcc
			288-294A-R	gcagccgctgcggcagctgcagcagtctcagctgatgaagc
			288-298PBS1-F	ggagacaaatctcatgtctcctcaggctatgtaagcaagcc
			288-298PBS1-R	ggagacatgagatttgtctccagcagtctcagctgatgaagc
			N5-283S-R	tgaagcagtcctattcagagcc
			283Y-F	tctgaataggactgcttcatacgctgagactgc
			N5-294G	agaaagtagtttatcagcagtctcag
			294Q-F	ctgctgataaactactttctcaggtttcaggctatgtaag
			N5-303Y-R	cacgtttggcttgcttacatag
			304S-F	gcaagccaaacgtgtccgaaatcgacgag
			N5-310AT-R	ttccattatctcgtcgatttcatacac
			311-2 IY-F	gaaatcgacgagataatggaaatctacaaggatttcagcgatgagtg

1099